

Western Indian Ocean marine and terrestrial records of climate variability: a review and new concepts on land–ocean interactions since AD 1660

J. Zinke · M. Pfeiffer · O. Timm · W.-Ch. Dullo ·
G. J. A. Brummer

Received: 18 December 2006 / Accepted: 13 August 2008 / Published online: 6 September 2008
© The Author(s) 2008. This article is published with open access at Springerlink.com

Abstract We examine the relationship between three tropical and two subtropical western Indian Ocean coral oxygen isotope time series to surface air temperatures (SAT) and rainfall over India, tropical East Africa and southeast Africa. We review established relationships, provide new concepts with regard to distinct rainfall seasons, and mean annual temperatures. Tropical corals are coherent with SAT over western India and East Africa at interannual and multidecadal periodicities. The subtropical corals correlate with Southeast African SAT at periodicities of 16–30 years. The relationship between the coral records and land rainfall is more complex. Running correlations suggest varying strength of interannual teleconnections

between the tropical coral oxygen isotope records and rainfall over equatorial East Africa. The relationship with rainfall over India changed in the 1970s. The subtropical oxygen isotope records are coherent with South African rainfall at interdecadal periodicities. Paleoclimatological reconstructions of land rainfall and SAT reveal that the inferred relationships generally hold during the last 350 years. Thus, the Indian Ocean corals prove invaluable for investigating land–ocean interactions during past centuries.

Keywords Coral oxygen isotopes · Terrestrial proxy records · Indian Ocean · Africa · India

Electronic supplementary material The online version of this article (doi:10.1007/s00531-008-0365-5) contains supplementary material, which is available to authorized users.

J. Zinke (✉)
Faculty of Earth and Life Sciences, Vrije Universiteit
Amsterdam, FALW, De Boelelaan 1085, 1081 HV, Amsterdam,
The Netherlands
e-mail: jens.zinke@falw.vu.nl

M. Pfeiffer
Institut fuer Geologie und Mineralogie, Universitaet zu Koeln,
Cologne, Germany

O. Timm
International Pacific Research Center, University of Hawaii,
Honolulu, HI, USA

W.-Ch. Dullo
Leibniz Institut fuer Meereswissenschaften, IFM-GEOMAR,
24148 Kiel, Germany

G. J. A. Brummer
Department of Marine Chemistry and Geology, Royal NIOZ,
Den Burg, Texel, The Netherlands

Introduction

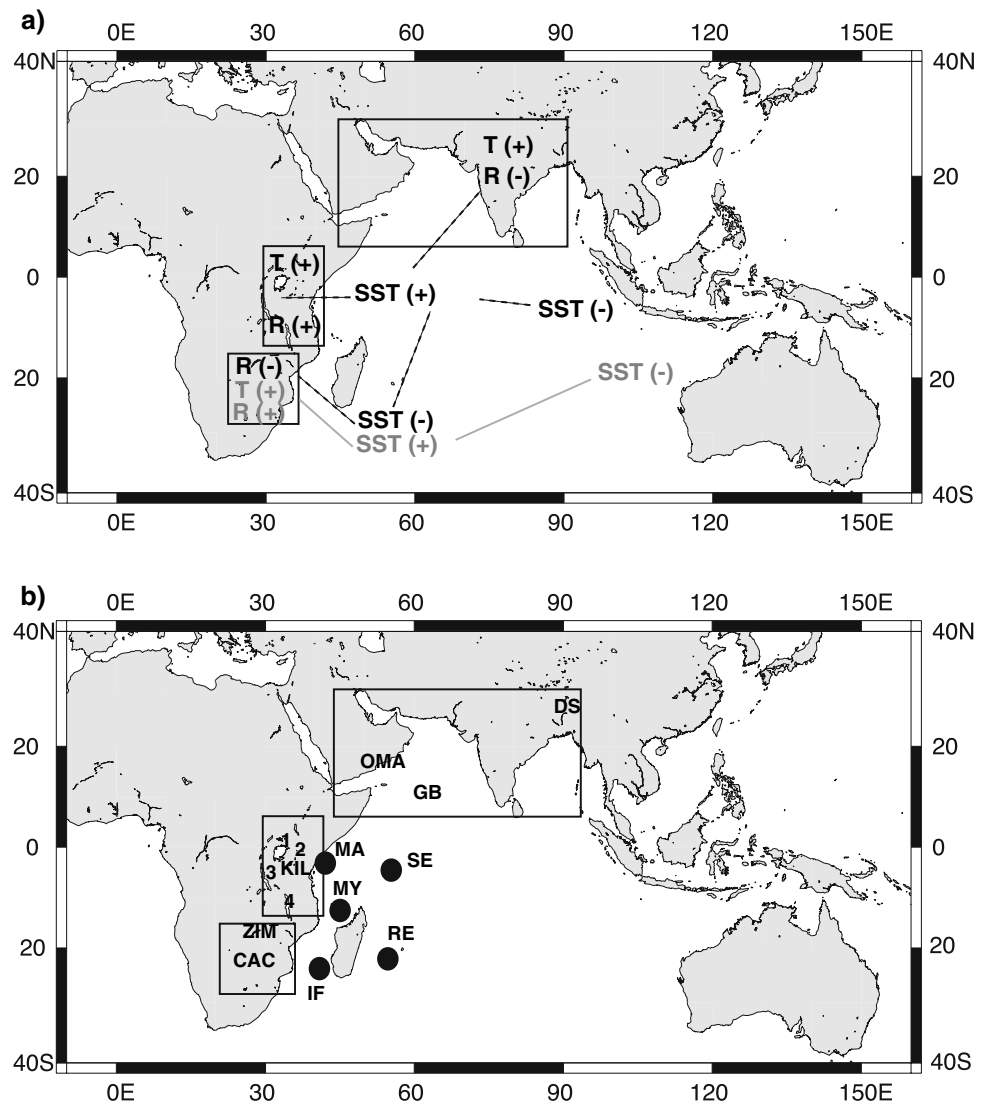
In light of rapidly changing boundary conditions caused by global warming, decadal to multidecadal climate variability has become a major focus of climate research. In this context, the impact of rising sea surface temperatures (SST) on surface air temperature (SAT) and rainfall over land is of primary importance. Kumar et al. (2004) showed that over last 50 years tropical surface temperatures and precipitation over land and oceans have differing trends. SAT over land increases in phase with the rising SSTs. In contrast, precipitation over land decreases with increasing precipitation over the oceans due to the warmer SSTs (Kumar et al. 2004). This unfortunate combination of increasing surface temperatures and decreasing precipitation over tropical land regions could combine to produce considerable societal consequences. Therefore, changing teleconnection patterns, such as the breakdown of the historical ENSO-Monsoon correlation in recent decades,

attracted considerable attention (Kumar et al. 1999). One reason for the very heterogeneous response of precipitation to rapidly warming tropical oceans is the non-linear relationship between SST and rainfall (e.g. Timm et al. 2005; Pfeiffer et al. 2006). In the tropical Indian Ocean, mean SSTs are high, and small changes may have a profound impact on precipitation (Timm et al. 2005).

Interannual to multidecadal variations have been found in drought and precipitation records around the globe (Dai et al. 1998; Shi and Chen 2004; D'Arrigo et al. 2005; Meehl and Hu 2006). The possible forcing factors for such variations were identified to originate from the Indo-Pacific and North-Atlantic oceans including the Pacific Decadal Oscillation (PDO, Mantua et al. 1997; Deser et al. 2004), the El Niño-Southern Oscillation (ENSO; McPhaden et al. 2006) and the Atlantic Multidecadal Oscillation (AMO) (McCabe and Palecki 2006). In addition, a tropical multidecadal mode (TMM) was described that captures most of

the variance in tropical surface temperatures and convection (Chelliah and Bell 2004). The variability in Indian Ocean SST's in concert with PDO and ENSO variability emerged to have a large influence on rainfall and temperatures on surrounding landmasses, i.e. India, East Africa, South Africa and Austral-Asia (Jury et al. 2002). Several studies revealed that the atmospheric response to Indian Ocean SST changes is essential for simulating observed rainfall variability over large parts of Africa (Goddard and Graham 1999; Latif et al. 1999; Clark et al. 2000; Richard et al. 2000; Reason and Mulenga 1999; Reason 2001; Reason and Rouault 2002; Jury et al. 2004; Vecchi and Harrison 2004). Whatever the dominant forcing of decadal variability, it is clear that certain Indian Ocean SST patterns are related to drought or rain excess in certain regions of Africa and India. The interaction between the Indian Ocean and the adjacent land regions is summarized in Fig. 1.

Fig. 1 a Schematic view of the relationship between surface air temperature (SAT) and rainfall over India and East Africa to tropical Indian Ocean sea surface temperature (SST) patterns (black) and southern subtropical Indian Ocean SST patterns to SAT and rainfall in Southern Africa; (+ positive anomaly; – negative anomaly). In grey tropical/subtropical SST gradient and its influence on rainfall in Southern Africa. The rectangular boxes indicate regions investigated in this article. b coral and terrestrial proxy locations studied; corals: MA Malindi (Cole et al. 2000), SE MAHE (Pfeiffer and Dullo 2006), MY Mayotte (Zinke et al. 2005), RE Reunion (Pfeiffer et al. 2004), IF Ifaty (Zinke et al. 2004a, b); terrestrial proxy sites: DSU Dasuopu Ice core (Thompson et al. 2003), OMA Oman stalagmite $\delta^{18}\text{O}$ (Burns et al. 2002), GB *G. bulloides* abundance Arabian Sea sediment core (Anderson et al. 2002), KIL Kilimanjaro Ice Core (Thompson et al. 2002), CAC Cold Air Cave (Holmgren et al. 1999), ZIM Zimbabwe Tree rings (Therrell et al. 2006); Lake records: 1 Lake Victoria (Stager et al. 2005), 2 Lake Naivasha (Verschuren et al. 2000), 3 Lake Tanganyika (Cohen et al. 2006), 4 Lake Malawi (Johnson et al. 2001)



Examining the relationship between tropical SST and land surface temperatures and precipitation on decadal scales is hindered by the relatively short observational database, particularly in the oceans. Proxy records can potentially extend the oceanic and land climate records far beyond instrumental data. Tree rings, lake sediment records and laminated stalagmites provide annually resolved proxy data for surface temperature and/or precipitation over the African-Asian landmass for several centuries (Fig. 1b; Holmgren et al. 1999; Tyson et al. 2002; Verschuren et al. 2000; Verschuren 2004; Burns et al. 2002; Cook et al. 2003; Deser et al. 2004; Fleitmann et al. 2004; D'Arrigo et al. 2005, 2006; Therrell et al. 2006 and references therein). Geochemical parameters in massive coral skeletons from the Indian Ocean are well established in providing monthly to annually resolved time series of changes in SST, salinity and precipitation in the shallow oceans for up to 350 years (Fig. 1b; Charles et al. 1997, 2003; Cole et al. 2000; Cobb et al. 2001; Kuhnert et al. 2000; Zinke et al. 2004a, b, 2005; Pfeiffer et al. 2004, 2006; Timm et al. 2005; Damassa et al. 2006).

This article uses the available Indian Ocean coral $\delta^{18}\text{O}$ records as proxy time series of SST, and compares their interannual to multidecadal variability to terrestrial time series (instrumental and proxy) (Fig. 1). We will focus on three regions where Indian Ocean SST's are known to be important for regional temperature and rainfall variability, (1) India, (2) Tropical East Africa and (3) Subtropical South-East Africa (Fig. 1). We aim to bring the observed trends between ocean and land climate as observed by Kumar et al. (2004) into a long-term context. Such a comparison is invaluable in addressing the question to what extent anthropogenic forced warming influenced decadal teleconnections.

The paper is structured as follows: we will initially describe the climate of the Indian Ocean regions studied in this article. We will continue with a description of the instrumental and coral data used, before examining the correlation of the coral records with land temperature and rainfall over the twentieth century. In Sect. 5 we will provide an outlook of how terrestrial and marine paleoclimate records can help to understand past variations in the land-ocean climate interaction.

Climate of the western Indian Ocean and adjacent continents

The climate of the regions surrounding the Indian Ocean is dominated by the Asian monsoon. The monsoon circulation is driven by the pressure gradients resulting from differential heating over the Eurasian continent and the Indian Ocean, modified by the rotation of the Earth

(Webster et al. 1998). The region influenced by the Asian monsoon is characterized by a seasonal reversal of surface wind fields and a distinct seasonality of precipitation. During the SW Monsoon (austral winter, June–September) India receives most of its total annual rainfall. During this time, the South Asian continent is very warm and large-scale atmospheric convection occurs over the continent. Over East Africa, the climatological evolution of rainfall is primarily controlled by the movements of the ITCZ from its position north of the equator in austral winter to its most southerly position in austral fall. For this reason, East Africa experiences two distinct rainy seasons, the short rains from October to December (OND) and the long rains from March to May (MAM). OND rainfall experiences larger interannual variability than the MAM rains (Hastenrath and Greischar 1993; Hastenrath and Polzin 2005). MAM rainfall is mainly dominated by tropical Atlantic Ocean variability (Mutai and Ward 2000). January to March (JFM) rainfall has also been in the focus of many studies (e.g. Hugh 2004). This season is considered the mean austral summer rainfall season where rainfall anomalies in East Africa between north and south of 10°S tend to oppose each other (Hugh 2004). The JFM season comprises important parts of rainfall seasons in central-east and southeastern Africa, which are closely linked to Indian Ocean SST. The mean austral summer season for southeast Africa south of 15°S is defined between December and March, when the ITCZ reaches its southernmost position.

The role of the distribution of SST in the Indian Ocean in determining monsoon rainfall variability over India is highly debated (Clark et al. 2000; Vecchi and Harrison 2004). High SST in the Arabian Sea precedes strong monsoon rain, which in turn precedes low SST in austral winter (Cherchi et al. 2007). The cooling in the western tropical Indian Ocean via wind-evaporation feedbacks is the strongest and homogeneously distributed across the western Indian Ocean (20°N – 5°S , 50 – 70°E) for the late Asian monsoon season (September–November, SON). Vecchi and Harrison (2004) identified two distinct regions with strong rainfall anomalies in the India Monsoon domain, Western Ghats and Ganges-Mahanadi Basin, which appear to be independent from each other. This implies different mechanisms that control rainfall variability in the two regions. Western Ghats SAT and rainfall shows the strongest relationship with Arabian Sea SST. On interannual and interdecadal time scales, the monsoon is linked with ENSO. The occurrence of El Niño is usually associated with a weak monsoon and La Niña with a strong monsoon (Webster et al. 1998). However, the relationship between the Asian Monsoon and ENSO is statistically non-stationary and a breakdown of the relationship after 1976 is observed (Kumar et al. 1999).

Rainfall over Eastern Africa is strongly correlated with the two dominant processes of interannual variability affecting the Indian Ocean SSTs, the Indian Ocean Zonal Mode (IOZM) and the El-Niño-Southern Oscillation (ENSO) (Ropelewski and Halpert 1987; Saji et al. 1999; Goddard and Graham 1999; Pocard et al. 2000; Black et al. 2003; Clark et al. 2003). The IOZM is originally defined as the difference in sea surface temperatures (SST) between an eastern (EIO) and western Indian Ocean (WIO) region during boreal fall, it is in its positive mode when WIO-SST are anomalously warmer than EIO-SST. The ENSO originates from the tropical Pacific and is defined as the globally leading interannual coupled atmosphere–ocean process increasing WIO-SST in austral spring and summer (McPhaden et al. 2006). Warm WIO-SST in response to these modes were found to correlate strongly with excess rainfall in the so-called East African short rains (hereafter EASR; from October to December Goddard and Graham 1999).

South Africa Rain is characterized by interdecadal variability between 16 and 20 years, which is observed in several studies of South African summer rainfall variability (Mason 1995; Krueger 1999; Reason et al. 1996; Reason 2002; Reason and Rouault 2002; Tyson et al. 2002; Jury et al. 2004). Warm (cool) SST anomalies in the southwestern Indian Ocean are associated with increased (decreased) rainfall over central and eastern South Africa on seasonal to interdecadal time scales. Several studies concluded that this interdecadal variability is modulated by ENSO-like decadal variability, which influences southern Indian Ocean SST and wind fields on multi-decadal time scales (Allan et al. 1995; Reason et al. 1996; Reason and Rouault 2002). Richard et al. (2000) proved that after the late 1960s, the influence of ENSO variability on South Africa rainfall increased, which is associated with a decrease in rainfall over certain areas. Reason and Rouault (2002) postulate that the remote influence of large-scale SST and sea level pressure (SLP) fields in the Indo-Pacific mainly influences the mean position of the

tropical temperature troughs, the main rain-producing systems, and therefore, the amount of rainfall received in particular areas across southern Africa. Williams et al. (2006) show evidence for such associations for the recent decade.

Instrumental data

Historical surface air temperatures (SAT) over land are derived from CRUTEM3 monthly mean temperature from the Hadley Center of the UK Meteorological Office on a $5^\circ \times 5^\circ$ grid-box basis for the period 1900–1995 (Table 1; Brohan et al. 2006). From CRUTEM3 we compute SAT over India covering $7.5\text{--}20^\circ\text{N}$, $72.5\text{--}77.5^\circ\text{E}$ representing the Western Ghats region. For tropical eastern Africa, we computed SAT covering $10^\circ\text{N}\text{--}15^\circ\text{S}$, $30\text{--}45^\circ\text{E}$ and for southern Africa covering $15\text{--}25^\circ\text{S}$, $20\text{--}45^\circ\text{E}$.

Historical monthly precipitation data are taken from the UEA CRU data product, which cover global land areas and extend over the time period from 1900 to 1998 (Hulme et al. 1998). The gridded data have a resolution of $2.5^\circ \times 3.75^\circ$ longitude. We averaged the precipitation data over the Western Ghats region ($7.5\text{--}20^\circ\text{N}$, $72.5\text{--}77.5^\circ\text{E}$), equatorial eastern Africa ($5^\circ\text{N}\text{--}5^\circ\text{S}$, $30\text{--}45^\circ\text{E}$) and southern Africa ($15\text{--}25^\circ\text{S}$, $20\text{--}45^\circ\text{E}$). Western Ghats rainfall was cross-checked with India Monsoon rainfall data per area provided by the Indian Institute of Tropical Meteorology for West Central India centered at 19°N , 78°E including 129 years of data between 1871 and 1999 (Parthasarathy et al. 1991, 1995; Sontakke and Singh, 1996). Both datasets, UEA CRU and IITM products show similar interannual and interdecadal variability (Suppl. Fig. S1).

Table 1 summarizes the instrumental data used in this study. For SAT, we use mean annual values, and for the rainfall, we average the data over the main rain producing seasons in the regions investigated. Major periodicities of SAT and rainfall variability described in the literature are also indicated.

Table 1 Regions and data sets used for the selected regions

| Region | Data set | Latitude-Longitude | Period | SAT | Prpc season | Periodicities years ^a |
|------------------|----------|---|-----------|-------------|-------------|----------------------------------|
| Western Ghats | UEA CRU | $7.5\text{--}20^\circ\text{N}$; $72.5\text{--}77.5^\circ\text{E}$ | 1900–1995 | – | JJA, SON | 2.7–3.3; 5–7; 9–14 |
| Western Ghats | CRUTEM3 | $7.5\text{--}20^\circ\text{N}$; $72.5\text{--}77.5^\circ\text{E}$ | 1900–1995 | Mean annual | – | 3.6; 5–6; 8–11; 18–25 |
| East Africa | UEA CRU | $5^\circ\text{N}\text{--}5^\circ\text{S}$; $30\text{--}45^\circ\text{E}$ | 1900–1995 | – | OND | 2.2; 3.3; 5–6; 18–25 |
| East Africa | UEA CRU | $5^\circ\text{N}\text{--}5^\circ\text{S}$; $30\text{--}45^\circ\text{E}$ | 1900–1995 | – | JFM | 4–6; 9–14 |
| East Africa | CRUTEM3 | $10^\circ\text{N}\text{--}15^\circ\text{S}$; $30\text{--}45^\circ\text{E}$ | 1900–1995 | Mean annual | – | 3.6; 4–6; 8–11; 45 |
| Southeast Africa | UEA CRU | $15\text{--}25^\circ\text{S}$; $20\text{--}45^\circ\text{E}$ | 1900–1995 | – | DJFM | 2.7; 3.7; 16–20 |
| Southeast Africa | CRUTEM3 | $15\text{--}25^\circ\text{S}$; $20\text{--}45^\circ\text{E}$ | 1900–1995 | Mean annual | – | 3.3; 4–6; 9–11; 16–30 |

The main rainfall seasons and the dominant periodicities significant above the 95% level for land temperatures and precipitation are indicated

^a The periodicities are calculated with MTM spectra from the original data. For references see text

Table 2 Linear correlation coefficients (r) between annual mean coral $\delta^{18}\text{O}$ and sea surface temperature (ERSST; Smith and Reynolds 2003) for a grid box including the individual coral sites for the time 1950–1995 and 1880–1995

| Coral core | ERSST 1950–1995 | P value | ERSST 1880–1995 | P value | Interannual (years) | Decadal (years) | References |
|------------|-----------------|-----------|-----------------|-----------|---------------------|-----------------|-------------------------|
| MAHE | −0.59 | 0.0001 | −0.69 | 0.0001 | 3.5; 4.7–5.8 | 10–16 | Pfeiffer and Dullo 2006 |
| NEP | −0.6 | 0.0001 | −0.57 | 0.0001 | 3.5; 5.5 | 9–13 | Pfeiffer and Dullo 2006 |
| BVB | −0.3 | 0.0001 | −0.62 | 0.0001 | 3.5–4; 5–5.5 | 11.8–12.3 | Charles et al. 1997 |
| Malindi | −0.36 | 0.0001 | −0.44 | 0.0001 | 3.5; 5.5 | 8–14 | Cole et al. 2000 |
| Mayotte | −0.31 | 0.01 | −0.33 | 0.0003 | 5–6 | 11–13; 25 | Zinke et al. 2005 |
| Ifaty | −0.63 | 0.001 | −0.33 | 0.001 | 3.9 | 16–18 | Zinke et al. 2004a, b |
| Reunion | −0.2 | ns | −0.2 | 0.03 | 3.7; 6.3–7.2 | 35 | Pfeiffer et al. 2004 |

The dominant interannual and decadal periodicities in the coral $\delta^{18}\text{O}$ records significant above the 95% level are indicated. References are indicated

A complete global SST dataset (ERSST) has been constructed by Smith and Reynolds (2003) based on COADS data (Woodruff et al. 1998). The ERSST product provides reconstructed SST anomalies for the global ocean interpolated over a $10^\circ \times 10^\circ$ grid. The monthly analysis begins in 1854, but the signal is dampened before 1880 due to sparse data (Smith and Reynolds 2003). We take the data for grid boxes centered at our various coral locations to groundtruth results obtained with our proxy data.

Coral data

The coral cores were drilled between 1994 and 2003 from massive colonies of the genus *Porites* sp. (*Porites lobata*, *Porites lutea*, *Porites solida*), using a commercially available pneumatic drill (Suppl. Inf. Tab 1; Zinke et al. 2005). The average growth rate of the corals sampled varied between 9 and 16 mm per year (Zinke et al. 2005). Thus, the 1 or 2 mm sample spacing provides approximately monthly or bimonthly resolution, respectively. We generate time series of coral $\delta^{18}\text{O}$ for annual mean and different seasons of the year that represent the main rainfall seasons investigated in this study [(January/February/March (JFM), September/October/November (SON), October/November/December (OND), December/January/February/March (DJFM)]. Details on the analytical procedures and data processing can be found in Zinke et al. (2005).

The coral records assembled here were collected from tropical to subtropical locations within the western Indian Ocean (Fig. 1; Suppl. Inf. Tab. 1). The tropical sites include the Seychelles, Kenya (Malindi; data from Cole et al. 2000) and Mayotte (Comoros) and the subtropical sites include La Réunion and Ifaty (Madagascar) (Fig. 1). From the Seychelles, two coral cores are available: BVB (Charles et al. 1997) and NEP (Pfeiffer and Dullo 2006). Coral data are available for download at the WDC database for paleoclimatology of the National Climatic Data Center

(Charles et al. 1997; Cole et al. 2000; Pfeiffer et al. 2004, 2006; Zinke et al. 2004a, b).

All coral oxygen isotope records used in this study show a significant correlation with regional and large-scale SST variability (Table 2; Charles et al. 1997; Cole et al. 2000; Zinke et al. 2005; Pfeiffer and Dullo 2006) with the possible exception of La Réunion, which shows a more complex, time-dependent correlation with regional SST variations (see also Pfeiffer et al. 2004 for a discussion). Thus, SST variability dominates the coral $\delta^{18}\text{O}$ records used in this study. A strong ENSO signal is observed in all records, in three cases related to SST anomalies and in two, the ENSO signal is proposed to arise from oceanic advection or changes in the hydrologic balance (Zinke et al. 2004a, b; Pfeiffer et al. 2004). Decadal variability is prominent in all coral records with a periodicity varying between 9 and 13 years in the tropical (10°N – 10°S , 40 – 70°E) and 16–35 years in the subtropical corals (15 – 30°S , 40 – 70°E) (Charles et al. 1997; Cole et al. 2000; Cobb et al. 2001; Zinke et al. 2004a, b; Pfeiffer et al. 2004; Pfeiffer and Dullo 2006; Suppl. Fig. S2 and S3).

For comparison with instrumental SAT, all coral records were normalized by subtracting their mean and dividing by their standard deviation. For comparison with rainfall data, the coral records were normalized and detrended. Our results were crosschecked by using the relevant instrumental SST data from the ERSST data set (Smith and Reynolds 2003).

We compute a tropical coral index from the Kenya (Malindi), Seychelles (MAHE) and Mayotte annual mean $\delta^{18}\text{O}$ records for the period 1801–1995. The mean series was made by first scaling the individual coral time series so that they had a mean of zero and a variance of one (i.e. standardized to z scores), and then averaging the normalized series. Simple averaging of all the coral records would result in a bias towards the time series with the highest variance. The two Seychelles records were combined into a single composite, as using each record on its own would have resulted in a bias to the Seychelles, which have been

sampled twice (Wilson et al. 2006). Between 1847 and 1866, the tropical coral index comprises only the Seychelles and Kenya records, while between 1800 and 1847 the Kenya record was used on its own.

Results

India monsoon region

In this section, we will investigate the relationship between coral proxy data, land temperatures and rainfall over India during the twentieth century. Vecchi and Harrison (2004) established the highest correlation between India monsoon rainfall and tropical Indian Ocean SST for the Western Ghats region only. Therefore, we focus on surface temperatures and rainfall from the Western Ghats region of India, and investigate the relationship between surface temperatures and rainfall with three tropical coral $\delta^{18}\text{O}$ time series from the western Indian Ocean that are located within the field of the highest correlation established by Vecchi and Harrison (2004), i.e. Kenya (Malindi), Seychelles (MAHE) and Mayotte.

Surface air temperature (Western Ghats)

At first, we investigate the relationship between SST and SAT over India (Western Ghats region). All western Indian Ocean coral $\delta^{18}\text{O}$ time series except Ifaty correlate with Indian SAT, as all show a consistent long-term warming throughout the twentieth century (Suppl. Tab. 2 and 3). We calculated an annual mean coral $\delta^{18}\text{O}$ index for the western tropical Indian Ocean based on the arithmetic mean of the individual records from Malindi, MAHE and Mayotte. This tropical coral index has the highest correlation with Western Ghats SAT (Suppl. Tab. 2 and 3; Fig. 2). Thus, the coral time series indicate increasing SST in concert with increasing SAT over the Western Ghats region of India in the course of the twentieth century. The 31-year running correlation between Western Ghats SAT and our tropical coral index shows that the interannual relationship remained stable throughout the twentieth century. Similar results were obtained using western Indian Ocean ERSST, averaged between 0 and 15°S, 40–60°E. We find coherent periodicities between the coral proxies, Western Ghats SAT on interannual time scales of 5–6 years and 3.7 years, and weaker on interdecadal periodicities in agreement with results obtained from instrumental SST (Fig. 2).

Asian monsoon rainfall (Western Ghats)

Western Ghats rainfall averaged from September to November (SON) is characterized by multidecadal

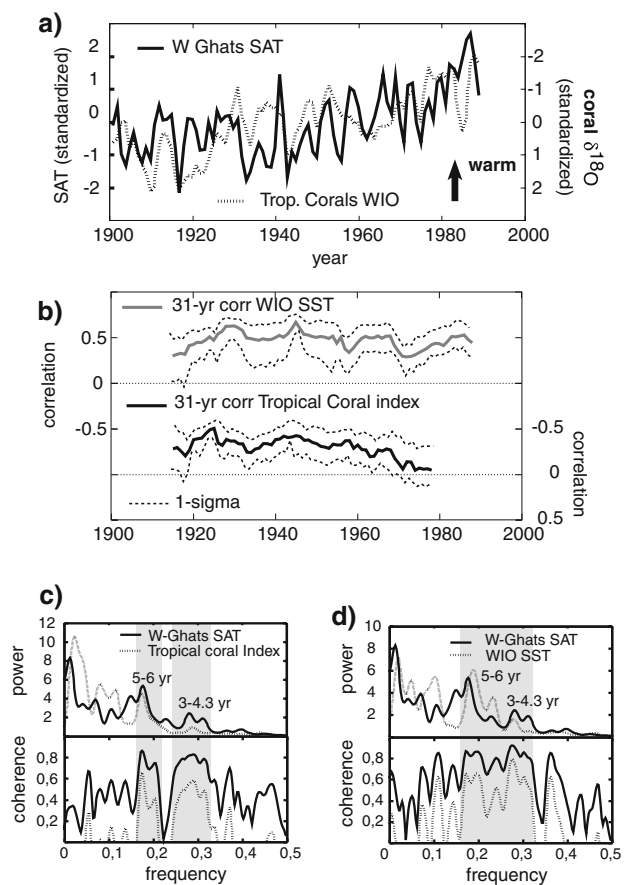


Fig. 2 **a** Time series of annual mean maximum surface air temperatures (SAT) for the Western Ghats region in India (Brohan et al. 2006) compared to the tropical coral $\delta^{18}\text{O}$ Index (see text for discussion) averaged from July to June. Negative anomalies in coral $\delta^{18}\text{O}$ correspond to warm SST. All time series were normalized by subtracting the mean and dividing by their standard deviation. Arrow indicates warm anomalies. **b** 31-year running correlation between July–June annual mean Western Ghats SAT and (top) ERSST (Smith and Reynolds 2003) averaged over the western Indian Ocean (WIO) 40–60°E, 0–15°S, and the tropical coral Index (bottom). All time series were detrended before analysis. 1-sigma confidence levels are indicated (dashed line). Correlation coefficients are plotted at the centre of each 31-year period. Correlation computed at <http://climexp.knmi.nl/>. **c** Cross-spectral analysis of Western Ghats SAT with the tropical coral Index (**c**) and with WIO-SST (**d**). Main frequencies significant above 95% are indicated (shaded rectangles)

fluctuations, no significant long-term trend is observed. We constructed an arithmetic mean of the two seasonally resolved coral time series from the Seychelles (MAHE) and Mayotte and calculated the SON values. This time series indicates that cool SON tropical SST anomalies are associated with surplus SON rainfall for most of the twentieth century (Fig. 3a; Suppl. Fig. S5). However, after the 1970s, this relationship changes. A 31-year running correlation between Western Ghats rainfall and the combined MAHE and Mayotte coral time series indicates a stable interannual relationship for most of the twentieth

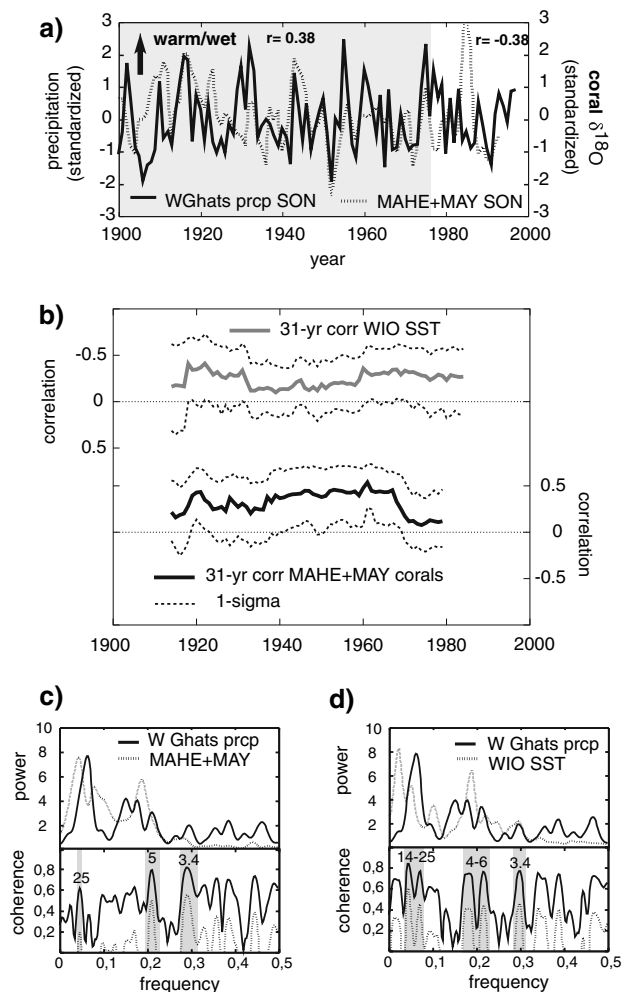


Fig. 3 **a** Time series of rainfall in the Western Ghats region India (7.5–20°N, 72.5–77.5°E; Hulme et al. 1998) averaged between September and November (SON) (*top*) compared to Seychelles and Mayotte (MAHE/MAY; *grey stippled*) coral $\delta^{18}\text{O}$ for SON. Negative anomalies in coral $\delta^{18}\text{O}$ correspond to warm SST. All time series were detrended and normalized by subtracting the mean and dividing by their standard deviation. *Arrow* indicates wet/warm anomalies. Note the change from positive (*grey bar*) to negative correlations after the 1970 s. **b** 31-year running correlations between SON Western Ghats rainfall and (*top*) Western Indian Ocean ERSST for SON (40–60°E, 0–15°S; *grey line*) and MAHE/MAY coral $\delta^{18}\text{O}$ for SON (*bottom*). All time series were detrended before analysis. 1-sigma confidence levels are indicated (*dashed line*). Correlation coefficients are plotted at the centre of each 31-year period. Correlation computed at <http://climexp.knmi.nl/>; **c** Cross-spectral analysis of SON Western Ghats rainfall with SON MAHE/MAY coral $\delta^{18}\text{O}$ (**d**) and with SON Western Indian Ocean ERSST (Smith and Reynolds 2003). Main frequencies significant above the 95% level are indicated (*shaded rectangles*)

century and a weakening of the relationship after the late 1970s (Fig. 3b). Instrumental SST also indicates a weak but stable interannual relationship. Cross-spectral analysis reveals that the combined MAHE and Mayotte coral $\delta^{18}\text{O}$ time series for SON is coherent with SON Western Ghats rainfall on interannual (5–6 years) and decadal (7–8 years

and 11–13 years) time scales (Fig. 3c). The strongest coherence is found at interannual time scales (5–6 years).

Discussion

Several authors have explored the relationship between All India Rainfall and coral time series of SST from the western equatorial Indian Ocean (Charles et al. 1997; Cole et al. 2000; Pfeiffer and Dullo 2006). However, a statistically significant relationship could not be observed (Cole et al. 2000; Pfeiffer and Dullo 2006). This study focuses on SAT and rainfall in the Western Ghats region of India, as this region has been shown to be much more sensitive to SST in the western Indian Ocean (Vecchi and Harrison 2004).

The relationship between mean annual Western Ghats SAT and the mean annual average coral record from the western equatorial Indian Ocean is fairly strong and stable over the twentieth century. Warmer SSTs are generally associated with higher SATs. This also holds on long time scales. Coherency is particularly high on interannual time scales and most likely reflects the impact of ENSO and/or the IOZM (Fig. 3).

The relationship between coral $\delta^{18}\text{O}$ and monsoon rainfall over the Western Ghats region of India is more complex. Correlations are highest for the late Asian monsoon season (SON) when the cooling in the western tropical Indian Ocean via wind-evaporation feedback is strongest and homogeneously distributed across the western Indian Ocean (20°N–5°S, 50–70°E; Vecchi and Harrison 2004). This suggests that the Indian Ocean SST in SON respond passively to the Asian Monsoon in that a stronger monsoon leads to stronger cooling in the tropics. This relationship is very stable throughout the twentieth century, with the exception of the late twentieth century. The strongest correlation with SAT and rainfall is observed with the Seychelles corals due to its position in the center of the cross-equatorial cell of the monsoon circulation. However, the SON time series calculated from both the Seychelles (MAHE) and Mayotte corals are coherent with rainfall in the Western Ghats region on decadal (11–13 years) and interannual (3–7 years) time scales. The interannual frequencies encompass the typical time scales of ENSO variability (e.g. Cole et al. 2000; Cobb et al. 2001; Pfeiffer and Dullo 2006). The tropical Pacific is known to have a strong influence on Indian Ocean SST and Indian monsoon rainfall and the correlation in both depends on the life cycle of ENSO. ENSO impacts on the strength of the Indian monsoon in its early phase, between August and November. El Nino (La Nina) events are typically associated with below-average (above-average) monsoon rainfall (e.g. Webster et al. 1998). The western Indian Ocean also responds to ENSO. ENSO-induced SST

anomalies develop in SON and reach their maximum in austral summer (January–April) of the following year, during the mature phase of ENSO. El Niño (La Niña) events are typically associated with warm (cold) SST anomalies. Hence, it is not clear whether the observed coherency between the coral records from the western Indian Ocean and rainfall in the Western Ghats region on interannual and decadal time scales reflects a direct climatic link or mainly results from the impact of ENSO on both regions.

Interestingly, the change of the correlation between the tropical Indian Ocean coral records and Western Ghats rainfall in the late 1970 (Fig. 3a) coincides with the observed break-down of the historical relationship between ENSO and All India rainfall (e.g. Webster et al. 1998; Kumar et al. 1999), which has been attributed either to changes in the mean climate (Webster et al. 1998; Kumar et al. 1999), or stochastic processes (Gershunov et al. 2001). However, at present, it is not clear whether the change in the relationship between the Western Indian Ocean coral record and rainfall in Western Ghats is simply a result of the breakdown of the ENSO-monsoon relationship, as the impact of ENSO on SST in the western Indian Ocean sector has remained stable during the entire twentieth century (e.g. Charles et al. 1997; Pfeiffer and Dullo 2006).

East Africa

Surface air temperatures

We investigated the relationship between our composite coral $\delta^{18}\text{O}$ index with East African SAT averaged over 10°N – 15°S , 30 – 45°E (Fig. 4a; Suppl. Fig. S4; Hulme et al. 1998). The coral index and East African SAT clearly covary throughout the twentieth century on multidecadal time scales ranging between 30 and 45 years (Fig. 4a). However, a 31-year running correlation between the coral index and East African temperatures shows that the correlation on interannual time scales breaks down before 1940 (Fig. 4b). Using instrumental SST, we find a similar break down as with coral $\delta^{18}\text{O}$ (Fig. 4b). Focusing on the period 1940–1993 only, the coral data are coherent with East African temperatures on interannual (3–6 years) and interdecadal (12, 45 years) frequencies consistent with results obtained from instrumental SST (Suppl. Fig. S3).

East African rainfall

The MAHE and Mayotte coral OND values are negatively correlated with OND rainfall between 5°N – 5°S and 30 – 45°E (Suppl. Fig. S5). However, the correlation is weak and only MAHE shows statistically significant correlations

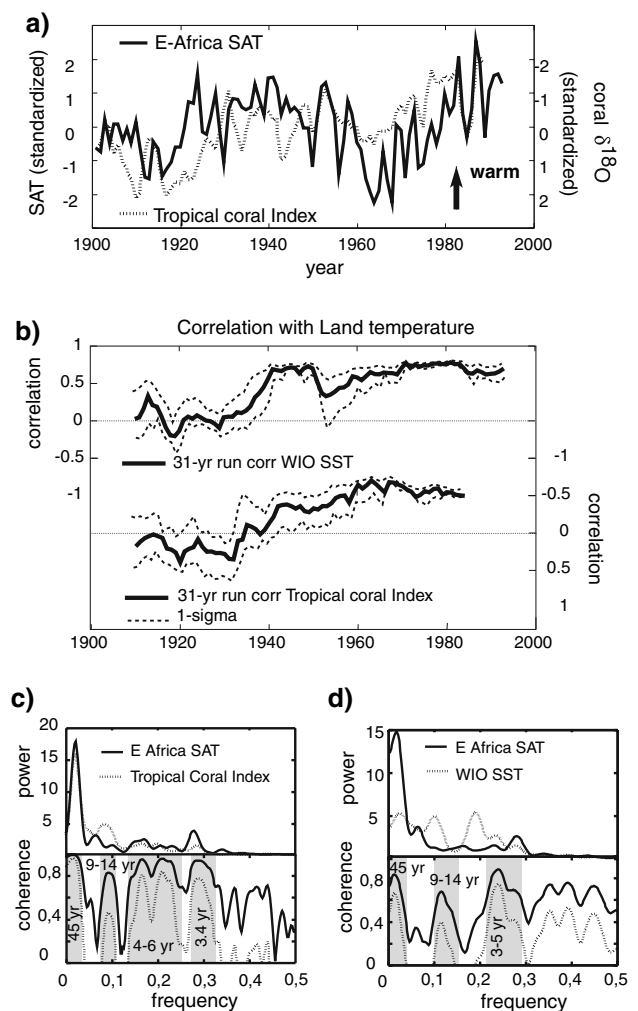


Fig. 4 **a** Time series of annual mean surface air temperatures (SAT) over East Africa (10°N – 15°S , 20 – 45°E ; Brohan et al. 2006) compared to annual mean tropical coral $\delta^{18}\text{O}$ Index (see text for discussion) averaged between July and June. Negative anomalies in coral $\delta^{18}\text{O}$ correspond to warm SST. All time series were normalized by subtracting the mean and dividing by their standard deviation. Arrow indicates warm anomalies. **b** 31-year running correlation between annual mean SAT over East Africa with (top) western Indian Ocean ERSST (Smith and Reynolds 2003; 40 – 60°E , 0 – 15°S) and (bottom) annual mean tropical coral $\delta^{18}\text{O}$ Index. All time series were detrended before analysis. 1-sigma confidence levels are indicated (dashed line). Correlation coefficients are plotted at the centre of each 31-year period. Correlation computed at <http://climexp.knmi.nl/>. **c** Cross-spectral analysis of East Africa SAT with tropical coral $\delta^{18}\text{O}$ Index (c) and with western Indian Ocean ERSST (d). Main frequencies significant above 90% level are indicated (shaded rectangles)

(Fig. 5a, b). A 31-year moving correlation between OND MAHE and East African rainfall indicates that negative correlations are observed for the early and late twentieth century (Fig. 5b). Western Indian Ocean SST (OND) shows similar, albeit slightly more stable temporal correlations. Cross-spectral analysis reveals that both MAHE and MAHE/Mayotte are coherent with East Africa Rainfall

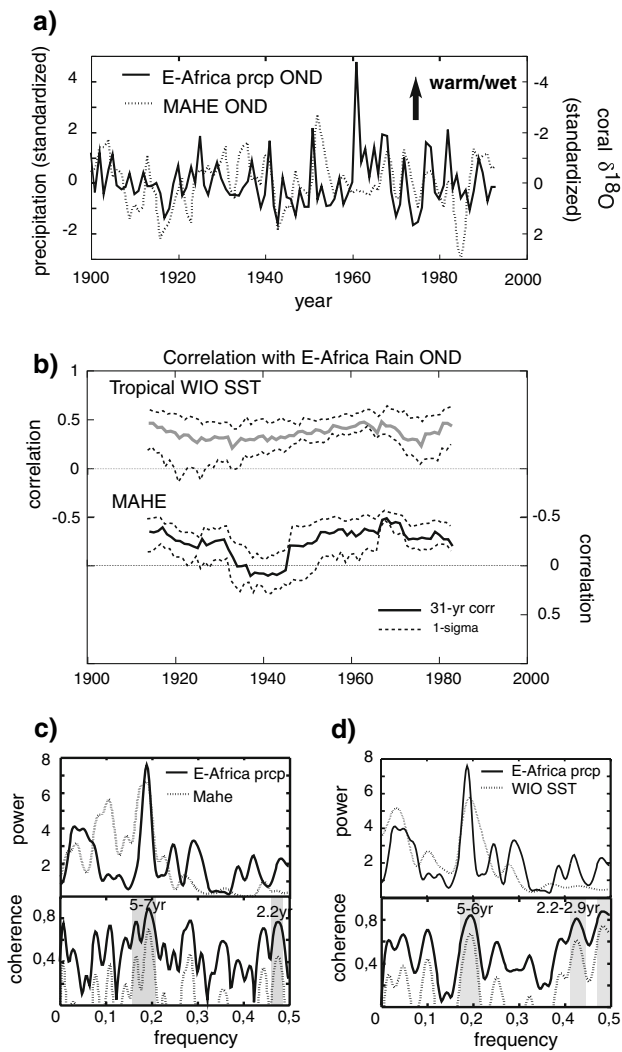


Fig. 5 **a** Time series of October to December (OND) East African Rainfall (5°N–5°S, 30–45°E; Hulme et al. 1998) compared to Seychelles (MAHE) coral $\delta^{18}\text{O}$ OND. Negative anomalies in coral $\delta^{18}\text{O}$ correspond to warm SST. All time series were normalized by subtracting the mean and dividing by their standard deviation. *Arrow* indicates wet/warm anomalies. **b** 31-year running correlation between East African rainfall for OND with (top) OND western Indian Ocean (WIO) ERSST (grey line) and (bottom) MAHE coral $\delta^{18}\text{O}$ for OND. All time series were detrended before analysis. 1-sigma confidence levels are indicated (dashed line). Correlation coefficients are plotted at the centre of each 31-year period. Correlation computed at <http://climexp.knmi.nl/>. **c** Cross-spectral analysis of East Africa Rainfall with MAHE coral $\delta^{18}\text{O}$ (c) and with WIO-ERSST (d) for the OND season. Main frequencies significant above the 90% level are indicated (shaded rectangles)

on interannual time scales of 5–6 years (Fig. 5c). Western Indian Ocean SSTs also indicate strong coherence on interannual and weaker coherence on decadal periodicities. Please note that the large rainfall event in 1961 is not recorded by the corals.

Mean austral summer rainfall over East Africa between JFM is positively correlated with Western Indian Ocean

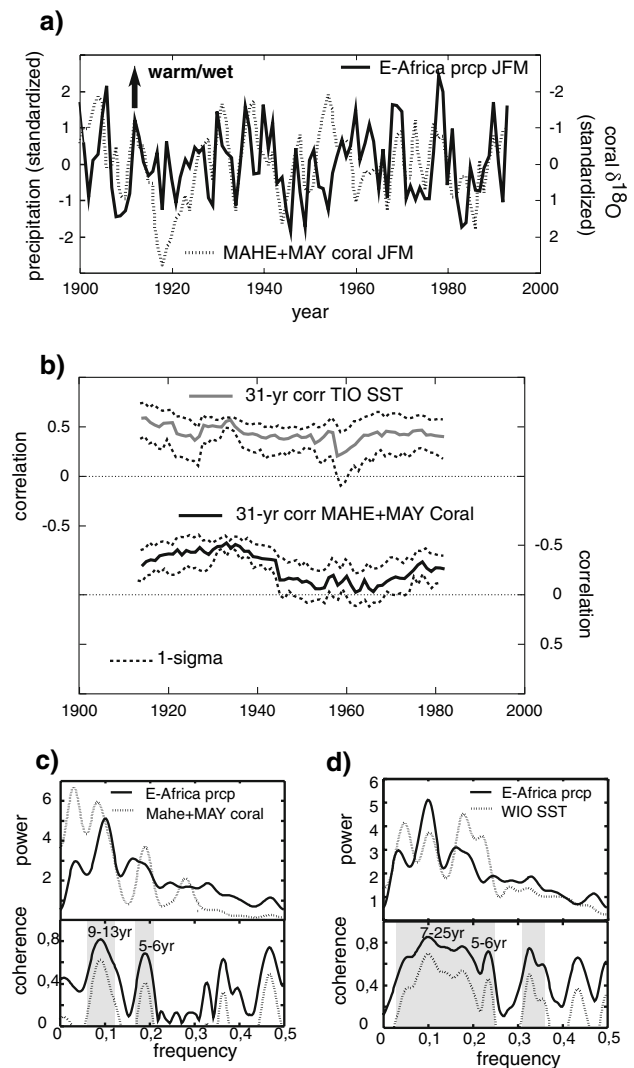


Fig. 6 **a** Time series of January to March (JFM) East African Rainfall (5°N–5°S, 30–45°E; Hulme et al. 1998) compared to Seychelles and Mayotte (MAHE/MAY) coral $\delta^{18}\text{O}$ for JFM. Negative anomalies in coral $\delta^{18}\text{O}$ correspond to warm SST. All time series were normalized by subtracting the mean and dividing by their standard deviation. *Arrow* indicates wet/warm anomalies. **b** 31-year running correlation between East African rainfall with (top) western Indian Ocean (WIO) ERSST (grey line; Smith and Reynolds 2003) and (bottom) MAHE/MAY coral $\delta^{18}\text{O}$ for JFM. All time series were detrended before analysis. 1-sigma confidence levels are indicated (dashed line). Correlation coefficients are plotted at the centre of each 31-year period. Correlation computed at <http://climexp.knmi.nl/>. **c** Cross-spectral analysis of East Africa Rainfall with MAHE/MAY coral $\delta^{18}\text{O}$ (c) and with WIO-ERSST (d) for the JFM season. Main frequencies significant above the 90% level are indicated (shaded rectangles)

SST for most of the twentieth century, with the exception of the mid-twentieth century (Fig. 6a, b; Suppl. Fig. S5). A similar temporal correlation is observed for the combined MAHE and Mayotte coral time series (Fig. 6b). Cross-spectral analysis between the corals and rainfall indicates a strong coherence on decadal and interannual periodicities

ranging between 9–13 and 5–6 years, respectively (Fig. 6c). Using instrumental SST, we obtain similar results. In contrast to the OND season, JFM rainfall has higher spectral power on decadal than on interannual periodicities (Suppl. Fig. S3). The same holds true for Western Indian Ocean SST and the combined coral index MAHE/Mayotte (Fig. 6d).

Discussion

Throughout the twentieth century, the tropical western Indian Ocean corals (and instrumental SST) follow SAT trends in East Africa (Suppl. Fig. S4). SAT and the coral index indicate periodic temperature variations with periodicities ranging between 30 and 45 years, although this signal is long, relative to the length of the time series investigated here. The 31-year running correlation clearly shows that the interannual relationship between western Indian Ocean SST and East Africa temperatures evolved and strengthened in the course of the twentieth century with the highest correlations in the last 50 years. As instrumental SST shows the same breakdown in the correlation with East African SAT prior to 1940, the observed change in relationship is unlikely to result from poor SST data or proxy data quality issues. We, therefore, speculate that the increase in the correlation between SAT and western Indian Ocean SST reflects the long-term warming trend in the region and possibly the increasing strength of ENSO. The prominent interannual and decadal periodicities found in the period after 1940 are consistent with the main frequencies reported for ENSO (Webster et al. 1998; McPhaden et al. 2006). In addition, the temporal correlation of the Nino3.4 Index with East Africa temperatures mimics the correlation indicated by the corals (Suppl. Fig. S6).

The relationship between the coral indices and East African rainfall is less clear (Suppl. Fig. S5). In general, warmer SSTs/more negative coral $\delta^{18}\text{O}$ in the western equatorial Indian Ocean are associated with higher rainfall over tropical East Africa, during the short rains (OND) as well as in the mean austral summer season (JFM). However, while instrumental SST from the tropical Western Indian Ocean indicates a stable correlation with East African rainfall over the twentieth century (Figs. 5b, 6b), the coral $\delta^{18}\text{O}$ time series also indicate periods with a weaker relationship, most notably in the 1930–1940 period (OND, Fig. 5b) and from the 1940–1970s (JFM, Fig. 6b).

The MAHE coral time series shows higher correlations with OND and JFM rainfall in East Africa than the combined MAHE/Mayotte time series. We note that a strong correlation between MAHE and OND precipitation appears in the late 1960s. Although instrumental SST indicates that our results must be viewed with some caution, we speculate

that the observed strengthening of the correlation may reflect the warming of the Indian Ocean in the second half of the twentieth century, as rainfall in equatorial East Africa strongly depends on Indian Ocean SSTs (e.g. Latif et al. 1999; Goddard and Graham 1999). Despite the weak linear correlation, the coral records indicate that tropical SST and East African rainfall are coherent on interannual time scales (5–6 years) for OND short rains and JFM mean austral summer rainfall. The decadal coherence is strong for JFM in a frequency band from 9 to 13 years. For OND, coral and rainfall time series indicate decadal (9–11 years) and multidecadal variability (18–30 years), but weaker coherence. These results agree with cross-spectral analysis of OND East Africa rainfall with western Indian Ocean SST (Fig. 5d). The periodicities found in the coral records probably indicate the influence of interannual and decadal ENSO variability on Indian Ocean SST and East African rainfall (e.g. Goddard and Graham 1999; Latif et al. 1999). Recently, Kayanne et al. (2006) found a strong relationship to East Africa rainfall in a 15-year-long monthly resolved coral $\delta^{18}\text{O}$ record from Malindi (Kenya), especially in Indian Ocean Zonal Mode (IOZM) years. A positive IOZM leads to warmer western Indian Ocean SST and easterly wind anomalies that favor strong precipitation events over tropical East Africa (Saji et al. 1999). Co-occurring IOZM and ENSO events as in 1997/1998 show the strongest response over the western Indian Ocean and eastern Africa (Behera et al. 2005). However, we note that the strong IOZM event which occurred in 1961 (e.g. Saji et al. 1999) is not recorded by the coral indices, although it led to extreme rainfall over East Africa during the OND short rains (Fig. 6a). Therefore, we conclude that longer monthly resolved coral records from offshore Kenya are needed in order to capture better the relationship between seasonal-scale SST anomalies in the western Indian Ocean and rainfall over East Africa.

Southeast Africa

Surface air temperatures

We selected the two subtropical Indian Ocean coral records from Ifaty (SW Madagascar) and La Réunion to investigate the link to southern African surface temperatures. Both subtropical coral records indicate a stable and significant correlation with southern African SAT on mean annual scales over the entire twentieth century (Suppl. Tab. 2 and 3; Fig. S4). However, we concentrate on the Ifaty record due to a dominant salinity signal on longer time scales in the La Réunion coral as indicated in Pfeiffer et al. (2004). The 31-year running correlation of the Ifaty coral $\delta^{18}\text{O}$ shows a stable correlation on interannual time scales, and these results are consistent with

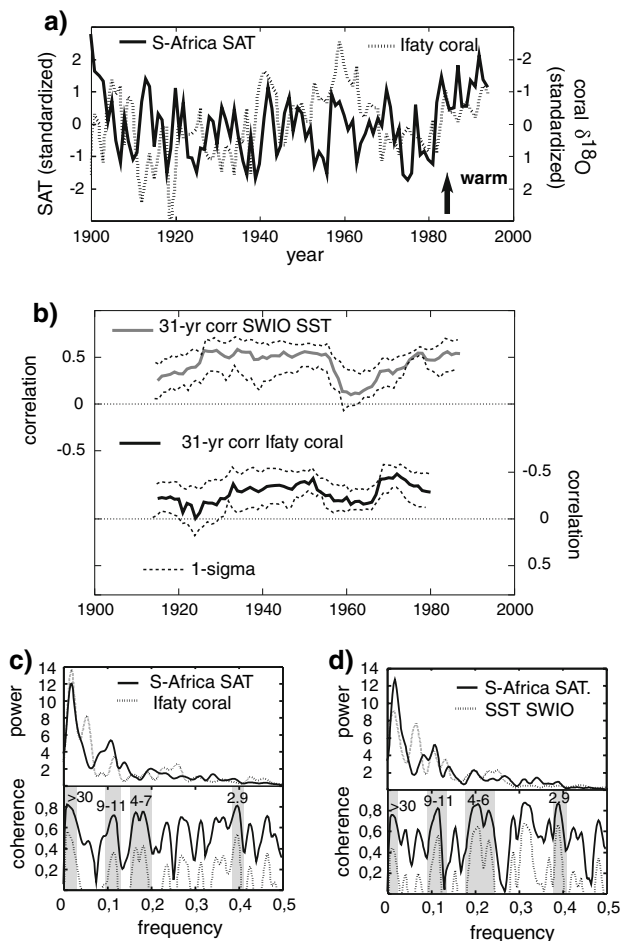


Fig. 7 **a** Time series of annual mean (March–February) surface air temperatures (SAT) over South East Africa (15–25°S, 20–45°E; Brohan et al. 2006) compared to mean annual Ifaty coral δ¹⁸O. Negative anomalies in coral δ¹⁸O correspond to warm SST. All time series were normalized by subtracting the mean and dividing by their standard deviation. *Arrow* indicates warm anomalies. **b** 31-year running correlation between annual mean South East Africa SAT with (*top*) southwestern Indian Ocean (SWIO) ERSST (*grey line*) and (*bottom*) Ifaty coral δ¹⁸O (*black line*). Time series were detrended before analysis. 1-sigma confidence levels are indicated (*dashed line*). Correlation coefficients are plotted at the centre of each 31-year period. Correlation computed at <http://climexp.knmi.nl/>. **c** Cross-spectral analysis of Southern Africa SAT with Ifaty coral δ¹⁸O (**c**) and with SWIO-ERSST (**d**). Main frequencies significant above the 90% level are indicated (*shaded rectangles*)

instrumental data of SST (Fig. 7a, b). We find coherent signals between the Ifaty coral record and southern African SAT on interdecadal (16–30 years) and interannual (4, 2–3 years) time scales (Fig. 7c). Using instrumental SST, we obtain similar results (Fig. 7d).

Southeast Africa rainfall

The mean austral summer season for southeast Africa south of 15°S is defined between December and March (Table 1). Southeast Africa rainfall in DJFM is characterized by

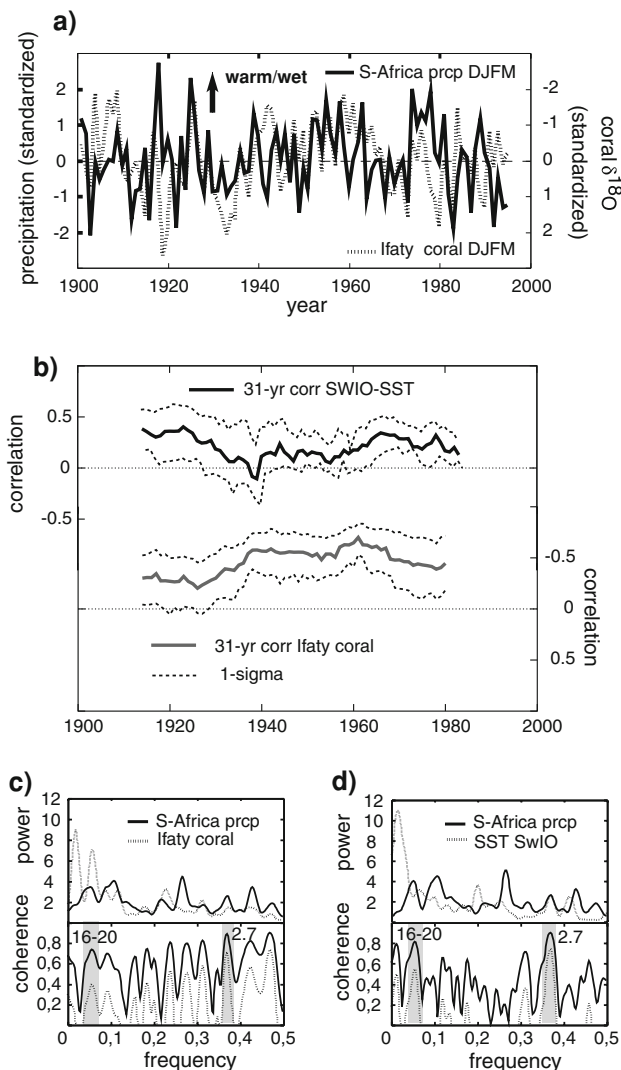


Fig. 8 **a** Time series of December to March (DJFM) South African summer rainfall region precipitation (15–25°S, 20–45°E; Hulme et al. 1998) compared to DJFM Ifaty coral δ¹⁸O (black stippled). Negative anomalies in coral δ¹⁸O correspond to warm SST. All time series were normalized by subtracting the mean and dividing by their standard deviation. *Arrow* indicates warm/wet anomalies. **b** 31-year running correlation between DJFM South East African rainfall with (*top*) southwestern Indian Ocean (SWIO) ERSST (*grey line*; Smith and Reynolds 2003) and (*bottom*) Ifaty coral δ¹⁸O (*black line*) for DJFM. Time series were detrended before analysis. 1-sigma confidence levels are indicated (*dashed line*). Correlation coefficients are plotted at the centre of each 31-year period. Correlation computed at <http://climexp.knmi.nl/>. **c** Cross-spectral analysis of Southern Africa Rainfall with Ifaty coral δ¹⁸O (**c**) and with SWIO-ERSST (**d**) for DJFM. Main frequencies significant above the 90% level are indicated (*shaded rectangles*)

multidecadal (30 years) and interdecadal fluctuations ranging from 16 to 20 years and interannual variability (2.9 and 3.6 years) (Fig. 8d). The DJFM series of the Ifaty coral record (as well as DJFM SSTs in the subtropical southwestern Indian Ocean, 30–60°E, 20–30°S) are coherent with South African Rainfall on interdecadal and interannual

periodicities ranging between 16 and 20 years, 3.2–3.6 and 2–2.7 years, respectively (Fig. 8c, d). A 31-year moving correlation between the DJFM Ifaty coral record and Southeast African rainfall is corroborated by the relevant historical SST record from the coral site (Fig. 8b). Note that the Ifaty coral even indicates a slightly more stable correlation over the course of the twentieth century.

Discussion

An important finding is that coral $\delta^{18}\text{O}$ for DJFM is coherent with south African SAT and with rainfall in the summer rainfall season on interdecadal (16–20 years) time scales. Subtropical southern Indian Ocean SST corroborates these findings. Significant interdecadal variability with periodicities between 16 and 20 years is observed in several studies of South African summer rainfall variability (Mason 1995; Krueger 1999; Reason and Rouault 2002; Tyson et al. 2002; Jury et al. 2004). Warm (cool) SST anomalies in the southwestern Indian Ocean are associated with increased (decreased) rainfall over central and eastern South Africa on seasonal to interdecadal time scales. Several studies concluded that this variability is modulated by interannual ENSO and ENSO-like decadal variability, which influences southern Indian Ocean SST, SLP and wind fields on multidecadal time scales (Allan et al. 1995; Reason et al. 1996; Richard et al. 2000; Reason and Rouault 2002). Zinke et al. (2004a, b) report interdecadal modulations of ENSO teleconnections in the Ifaty-4 coral time series throughout the twentieth century supporting the hypothesis of Indo-Pacific interactions on interdecadal time scales.

On the long-term, our coral data indicate that southern Africa summer rainfall decreased after the 1970s in response to the recent warming of the southwestern Indian Ocean and over southern Africa. This agrees with the observed response of the subtropical African regions to recent global warming (Hoerling et al. 2006).

Summary of coral–climate teleconnections in the twentieth century

The western Indian Ocean tropical and subtropical corals follow trends in SAT in West India, East Africa and South Africa and show coherence on interannual to multidecadal time scales over the twentieth century (Suppl. Fig. S4). The relationship between western Indian Ocean SST and rainfall over adjacent land areas is more complex (Suppl. Fig. S5). We find evidence for strong coherence between ocean temperatures and land rainfall on interannual time scales, most possibly associated with the strong ENSO teleconnection of the Indian Ocean. For the Indian Monsoon region, we observe changing teleconnection patterns on

interdecadal time scales probably linked to changes in the background SST through time. Our results are groundtruthed with instrumental data taken from the ERSST dataset (Smith and Reynolds 2003).

Land–ocean interaction from paleoclimatic records covering the past 350 years: an outlook

In this section, we will compare the coral records from the western Indian Ocean with other paleoclimatological records from the monsoon region, such as stalagmites, lake levels, sediments and ice cores. For this comparison, we use the tropical coral index, which extends back until 1801. The tropical coral Index will be compared with paleorecords from India and equatorial East Africa. For South East Africa, we use Ifaty only.

A comparison of various paleo-records is complicated by the fact that each paleoclimatic archive comes with a different temporal resolution ranging from annual to multidecadal and with a different age model uncertainty. Only tree ring chronologies have clear annual growth rings and age models as precise as corals. Nevertheless, we will show that major climatic trends can be traced in various archives, and that most of the relationships established for the twentieth century hold for the past 350 years.

Indian Monsoon region Paleo-records

Very few multicentury proxy records with annual or decadal resolution are available to investigate the land–ocean interaction on multidecadal-centennial scales for the Asian summer monsoon (Austral winter). The best available record for Asian Monsoon rainfall is a 780-year long stalagmite from Oman, which was shown to co-vary with summer monsoon rainfall over southern Arabia (Fig. 9a; Burns et al. 2002; Fleitmann et al. 2004). Rainfall over Oman shows a similar trend as western India rainfall for most of the twentieth century and thus, it provides an excellent paleo-record to study long-term rainfall changes in the Asian Monsoon domain. The relationship with Indian summer monsoon rainfall (Western Ghats) established for the twentieth century is successfully reproduced when we compare the tropical coral Index (back to 1801) with the Oman speleotheme reconstruction (Fig. 9a, d). The long-term decline of monsoonal rainfall in the twentieth century as observed in the Oman speleotheme is associated with a long-term warming of the Indian Ocean. In addition, we observe a negative correlation between the mean annual coral Index and speleotheme oxygen isotopes indicating that cooler tropical SSTs are associated with higher rainfall over Oman. This conclusion agrees with earlier studies by Burns et al. (2002) and Fleitmann et al.

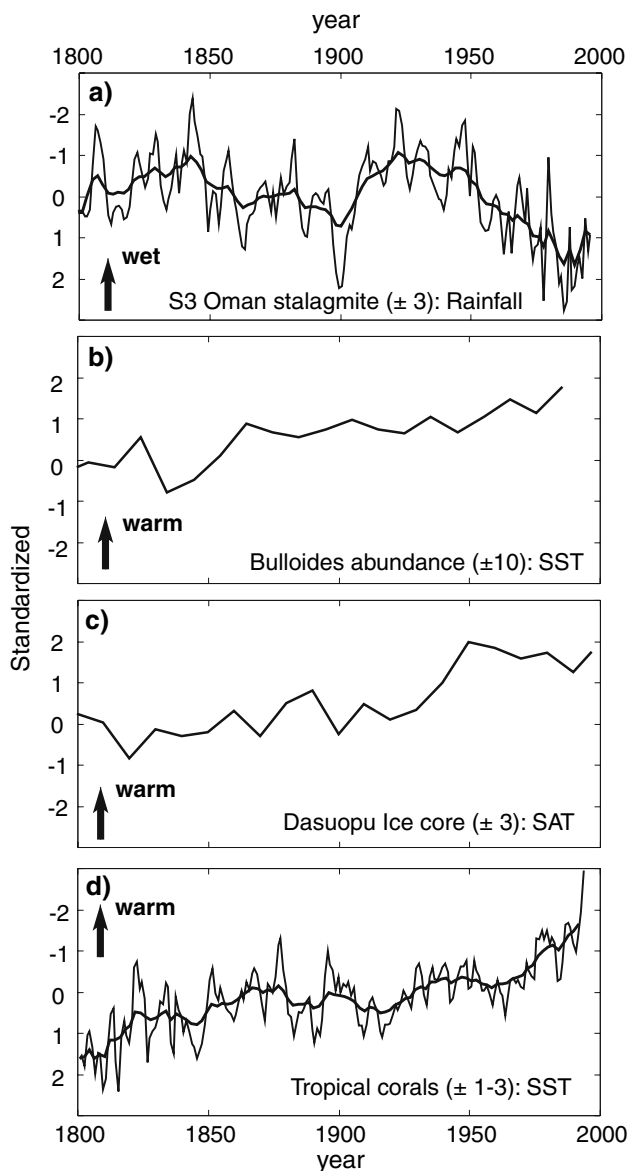


Fig. 9 Comparison of Indian Monsoon land surface proxy records with the tropical coral Index (see text for discussion). All time series were normalized by subtracting the mean and dividing by their standard deviation. Arrow indicates warm/wet anomalies. Age model uncertainties of individual records are indicated in brackets. **a** Oman stalagmite $\delta^{18}\text{O}$ with negative anomalies indicating wet conditions (Burns et al. 2002); **b** abundance of *G. bulloides* in Arabian Sea sediment core with high abundances indicating warm SST (Anderson et al. 2002); **c** Dasuopu Ice core $\delta^{18}\text{O}$ with positive anomalies indicating warm SAT (Thompson et al. 2003); **d** Tropical coral Index with negative anomalies indicating warm SST (this study). SST sea surface temperature, SAT surface air temperature

(2004). Interestingly, the abundance record of *G. bulloides* in a sediment core from the western Arabian Sea (Anderson et al. 2002), interpreted as an indicator of Asian Monsoon strength, is out of phase with the Oman speleotheme record, but largely in phase with our mean annual western Indian Ocean corals. This indicates that the

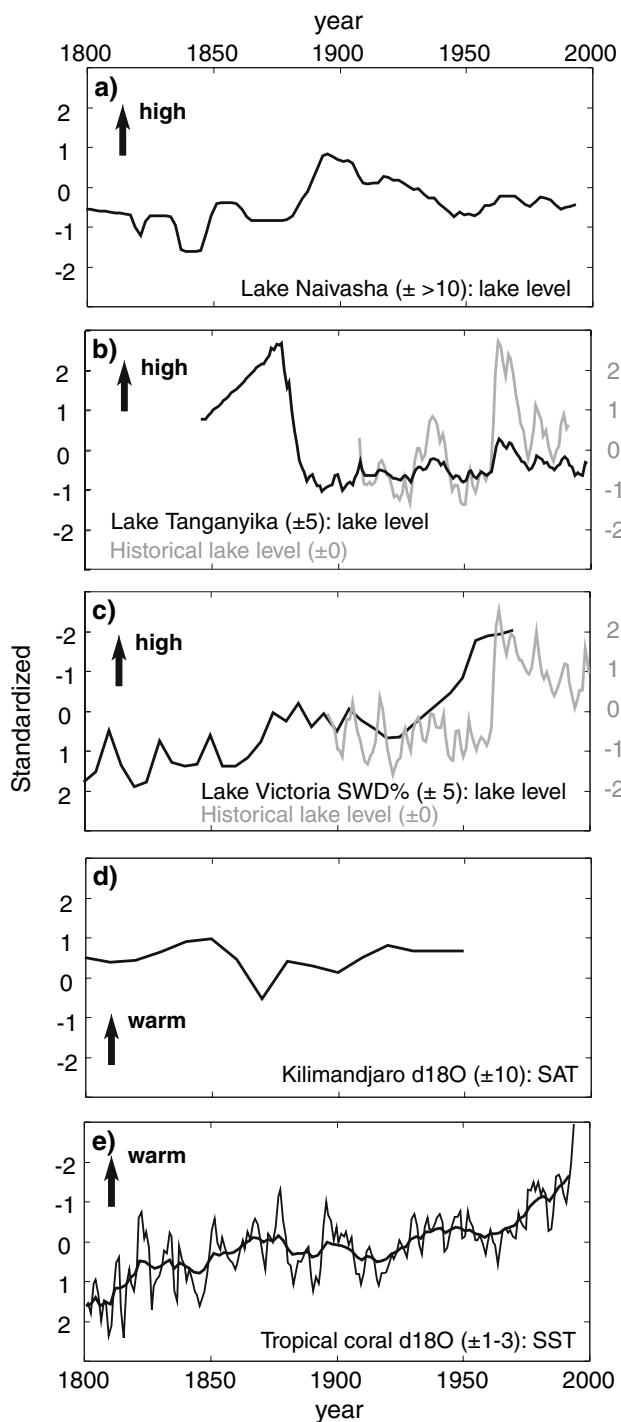
G. bulloides record rather reflects a mixture of summer and winter monsoon climate (SST) than a peak summer monsoon signal.

To date, no temperature reconstruction for the Indian Monsoon region is available, but several temperature and rainfall reconstructions for the Tibetan plateau can be found (e.g. Thompson et al. 2002; Cook et al. 2003; D'Arrigo et al. 2006; Treydte et al. 2006). We selected the Dasuopu ice core, which provides temperature variations over high Asia (Fig. 9b; Davis et al. 2005; Thompson et al. 2002, 2003). Mean annual surface temperature for High Asia in the Dasuopu ice core shows a long-term increase with highest temperatures in the twentieth century. The tropical Indian Ocean coral time series show a long-term warming of tropical Indian Ocean SST largely in-phase with Dasuopu (Fig. 9b). Dasuopu indicates a warming trend of SAT between 1800 and 1900 followed by a short cooling period in the early twentieth century, and then an accelerated warming trend in the second half of the twentieth century. Recently, D'Arrigo et al. (2006) compiled several tree ring temperature reconstructions for Eurasia that are within or at the edge of the Asian monsoon region. They show evidence for anomalous warming and increased precipitation over the Tibetan plateau in the twentieth century. D'Arrigo et al. (2006) proposed that the change in Eurasian land/tropical ocean temperature gradient is coupled to an intensified Asian monsoon over the Tibetan plateau. We observe a strong link between our tropical Indian Ocean corals and SAT over the Tibetan Plateau.

Interestingly, the warm tropical SSTs, as inferred from our tropical coral Index, and temperatures over inner Asia between 1960 and 1990 are associated with lower Monsoon rainfall at Oman, while precipitation increased over the Tibetan Plateau (High Asia) and across inner Asia (D'Arrigo et al. 2006; Treydte et al. 2006 and references therein). These results mark the highly non-linear response of the climate system to anomalous warming in the twentieth century in the Asian Monsoon region.

East Africa Paleo-records

Very few multicentury proxy records with annual or decadal resolution are available from East Africa to study the land–ocean interaction on multidecadal–centennial time scales. For East Africa we can use decadal resolved lake level reconstructions from various lakes in the East African Rift valley, which show a link to rainfall variability or moisture balance in that region over more than 350 years (Verschuren et al. 2000; Verschuren 2004 and references therein; Fig. 10a–c). Various proxies were used which are sensitive to lake level changes, each comes with a different temporal resolution and age model uncertainty (for a detailed discussion see Verschuren 2004). The Kilimanjaro



◀ **Fig. 10** Comparison of East African land surface proxy records with the tropical coral Index (see text for discussion). All time series were normalized by subtracting the mean and dividing by their standard deviation. *Arrow* indicates warm/wet anomalies. Age model uncertainties of individual records are indicated in brackets. **a** Lake Naivasha lake level in meters above sea level from sedimentation history (Verschuren et al. 2000); **b** Lake Tanganyika lake level in meters above sea level from ostracode assemblages (*black line*, Alin and Cohen 2003) and historical lake level in meters above sea level (*grey line*, Birkett et al. 1999); **c** Lake Victoria abundance of shallow water diatoms (SWD%; Stager et al. 2005) with lower abundances indicating higher lake level and historical lake level in meters above sea level (*grey line*, Tate et al. 2004); **d** Kilimanjaro Ice core $\delta^{18}\text{O}$ with positive anomalies indicating warm SAT (Thompson et al. 2002); **e** Tropical coral Index with negative anomalies indicating warm SST (this study). *SST* sea surface temperature, *SAT* surface air temperature

(Tanzania) ice core $\delta^{18}\text{O}$ record is the only terrestrial proxy record that is interpreted to reflect mainly temperature variations (Fig. 10e; Thompson et al. 2002).

East African lakes are known to be very sensitive to climate variations (Mercier et al. 2002; Bergonzini et al. 2004). Fluctuations in lake level mainly reflect changes in precipitation and evaporation integrated over the lake catchment area. The historical lake level trends in equatorial East Africa show strong similarities (Lake Victoria,

Lake Naivasha, Lake Turkana, Lake Bogoria and Lake Baringo; Verschuren et al. 2004). Most lakes show a major highstand between 1880 and 1920, a long decline to a lowstand in the 1950s and recovery thereafter (Verschuren 2004; Cohen et al. 2006). We selected Lake Naivasha, Tanganyika and Lake Victoria representative for historical lake levels in many equatorial East African lakes (Fig. 10a–c). Lake Naivasha shows a different long-term trend, indicating a broader highstand between 1890 and 1940 bracketed by lower lake levels (Fig. 10a; Verschuren 2004). Between 1870 and 2000, Lake Tanganyika and Lake Victoria lake level reconstructions agree, indicating the lowest levels in the first half of the twentieth century and high lake levels between 1870 and 1920 (Alin and Cohen 2003; Stager et al. 2005). Both Lake Victoria and Lake Tanganyika show a sudden jump to higher lake levels in the early 1960s (Birkett et al. 1999; Tate et al. 2004). The tropical Indian Ocean corals broadly follow long-term lake level variations over the nineteenth and twentieth century, although the sudden jump to higher lake levels in the early 1960s has no equivalent in the coral records (Fig. 10d). Therefore, this jump in lake level cannot be explained as a linear response to tropical SST warming. Rainfall station data from East Africa agree with lake level fluctuations on multidecadal time scales, with on average higher precipitation in the early and late twentieth century and a drier period in between.

The inferred temperature trends from Kilimanjaro ice $\delta^{18}\text{O}$ are broadly consistent with SST changes indicated by the tropical corals between 1800 and 1950: a long-term warming trend in the nineteenth century is followed by a short period of cooling in the late nineteenth/early twentieth century (Fig. 10d, e). Unfortunately, no temperature trend can be deduced from the Kilimanjaro ice core record for the late twentieth century. The Kilimanjaro record shows little coherence with East African lake level records. The East African lake level variations are probably not a simple response to SST changes in the tropical Indian Ocean.

Rather, they appear to be related to changing north–south SST gradient in the Indian Ocean that might control the moisture availability over the African Rift valley. Such a mechanism was proposed by Hoerling et al. (2006) and Jury et al. (2002). The reality of such a mechanism is observed for the early nineteenth century. Lowest lake levels on record are observed between 1800 and 1850, when warm subtropical Indian Ocean SST were associated with cooler tropical SST as indicated by the different trends in the Ifaty and the tropical coral Index (compare Fig. 10e and 11d).

Southeast Africa paleo-records

For southern Africa, a decadal resolved speleothem $\delta^{18}\text{O}$ record from Makapansgat Valley (3,000 years) was interpreted to reflect a combination of mean annual temperature and rainfall variability in South Africa (Fig. 11a; Holmgren et al. 1999; Tyson et al. 2002). A lake level record is available from Lake Malawi with annual resolution for the period 1650–1990 (Fig. 11b; Owen et al. 1990; Johnson et al. 2001). A tree ring record from Zimbabwe provides an annually resolved southern Africa summer rainfall reconstruction for November–February for the period 1796–1998 (Therrell et al. 2006; Fig. 11c).

The Ifaty-4 coral time series is the most robust subtropical Indian Ocean SST record and shows excellent agreement on the long-term trend with the Cold Air cave speleothem $\delta^{18}\text{O}$ record from Makapansgat Valley (Cold Air Cave; hereafter CAC) from South Africa (Fig. 11a, d). On multidecadal time scales, we observe an anticorrelation with the CAC speleotheme. This would suggest that warmer SSTs are associated with wetter conditions at CAC (Holmgren et al. 1999). For the Late Maunder Minimum (1675–1715) drier conditions at CAC are associated with cooler SST at Ifaty. The CAC stalagmite shows a dominant 16–20 year periodicity similar to the Ifaty coral. Trends in lake level fluctuations in Lake Malawi show good agreement for most of the 350 year record with the Ifaty coral (Fig. 11b, d; Johnson et al. 2001). Warm subtropical SSTs are associated with higher lake levels and vice versa. The CAC stalagmite co-varies with the Lake Malawi record for most of the 350 years (Fig. 11a, b). This confirms that a large fraction of the stalagmite record is related to the hydrologic conditions over Southeast Africa (Holmgren et al. 1999).

The comparison with the Zimbabwe rainfall reconstruction based on tree ring chronologies shows an anticorrelation on multidecadal time-scales with the annual mean Ifaty coral record (Fig. 11c, d). Cross-spectral analysis indicates that the Zimbabwe rainfall reconstruction is coherent with the Ifaty-coral time series on multidecadal (50–60 year), interdecadal (16–20 years) and interannual frequencies (2–3.5; not shown). This agrees with the dominant time scales of variability observed in instrumental

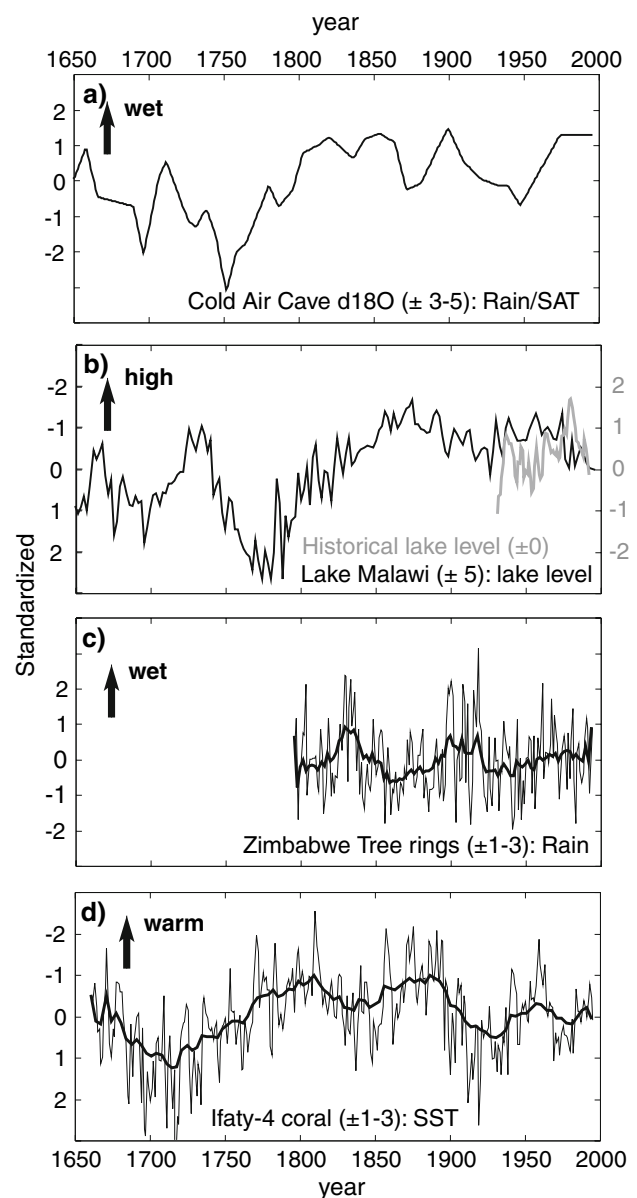


Fig. 11 Comparison of South African land surface proxy records with the Ifaty coral record. All time series were normalized by subtracting the mean and dividing by their standard deviation. Arrow indicates warm/wet anomalies. Age model uncertainties of individual records are indicated in brackets. **a** Cold Air Cave stalagmite $\delta^{18}\text{O}$ with positive anomalies reflecting wet/cool conditions (Holmgren et al. 1999); **b** Lake Malawi weight percentage of biogenic silica with lower percentages reflecting higher lake level (black line; Johnson et al. 2001) and historical lake level in meters above sea level (grey line; Owen et al. 1990); **c** Zimbabwe Tree-ring based rainfall reconstruction (Therrell et al. 2006); **d** Ifaty coral $\delta^{18}\text{O}$ with negative anomalies reflecting warm/wet conditions (Zinke et al. 2004a, b)

rainfall data from Southeast Africa from the twentieth century and in the Ifaty coral. Most of the interdecadal dry spells observed in the Zimbabwe rainfall reconstruction are associated with warm SST anomalies in the southern subtropical Indian Ocean.

Thus, for the last 350 years, our coral record off Madagascar indicates that the rainfall trends over southern Africa largely follow SST trends in the western Indian Ocean.

Conclusions

In this study, we established the interannual to centennial linkages between three tropical and two subtropical western Indian Ocean coral $\delta^{18}\text{O}$ time series to land temperatures and rainfall over India, equatorial East Africa and southeast Africa.

The western Indian Ocean tropical and subtropical corals show a strong correlation with land temperatures on interannual to multidecadal time scales. Tropical western Indian Ocean corals show clear decadal linkages at frequencies ranging from 7–13 to 30–45 years with temperatures over western India and East Africa back to 1800. The subtropical corals follow southern Africa SAT trends over more than 300 years, and are coherent with surface air temperatures on interdecadal frequencies ranging between 16 and 20 years.

The relationship between western Indian Ocean SST and rainfall over adjacent land areas is more complex. Running correlation analysis suggests varying strength of the interannual relationship. We find evidence for changing teleconnection patterns between SST/land temperatures and rainfall on interdecadal time scales, possibly associated with changes in the background temperatures through time. The most prominent change occurred in the late twentieth century, when teleconnection patterns changed dramatically. Nevertheless, three tropical Indian Ocean corals are coherent with equatorial East African rainfall on interannual (5–6 years) and decadal (9–13 years) frequencies, the main modes of interannual (ENSO) and decadal (ENSO-like) climate variability in the tropical Indo-Pacific. The subtropical corals indicate strongest coherence with southern African rainfall on interannual and interdecadal frequencies ranging between 2–3, 5–6 and 16–20 years, respectively.

Overall, this study reveals the great potential of tropical and subtropical Indian Ocean corals for reconstructing the complex relationship between tropical surface air temperatures and precipitation over land and oceans during the twentieth century and potentially beyond. This will provide a framework for a detailed analysis of decadal to multidecadal interactions between land and ocean at time scales well beyond the instrumental record.

Comparison with paleoclimatological reconstructions of either rainfall or temperature over land areas reveals that most relationships established for the twentieth century, also hold for the last 350 years. Thus, we believe that the network of high-resolution proxy records from the Indian

Ocean and the surrounding land mass will prove invaluable for a better understanding of land-ocean interactions over several centuries.

Acknowledgments We would like to thank the TESTREEF-group (contract Nr. EV5 V-CT 94-0447) for the drilling of the coral cores between 1994 and 1996. We especially thank B. Thomassin for his enthusiastic support. We thank DAF/SPEM Mayotte, Université de La Réunion and Centre d'Océanologie Marseille for supporting our field campaigns and the CITES permits. We thank H. Erlenkeuser (Leibniz Laboratory, University Kiel) and M. Joachimski (University Erlangen) for carrying out part of the oxygen isotope analysis. This research was supported by the German Science Foundation (Leibniz Award to Prof. Wolf-Christian Dullo and SFB 460, project B1), the Dutch NWO-ALW grant (awarded to Jens Zinke, grant number 854.00.034) and the European Community's Human Potential Programme under contract HPRN-CT-2002-00221 (STOPFEN). O. Timm was supported by the Japan Agency for Marine-Earth Science and Technology (JAMSTEC) through its sponsorship of the International Pacific Research Center. This is IPRC contribution number 547.

Open Access This article is distributed under the terms of the Creative Commons Attribution Noncommercial License which permits any noncommercial use, distribution, and reproduction in any medium, provided the original author(s) and source are credited.

References

- Alin SR, Cohen AS (2003) Lake-level history of Lake Tanganyika, East Africa, for the past 2500 years based on ostracode-inferred water-depth reconstruction. *Palaeogeogr Palaeoclimatol Palaeoecol* 199:31–49. doi:10.1016/S0031-0182(03)00484-X
- Allan RJ, Lindsay JA, Reason CJC (1995) Multidecadal variability in the climate system over the Indian Ocean region during the austral summer. *J Clim* 8:1853–1873. doi:10.1175/1520-0442(1995)008<1853:MVITCS>2.0.CO;2
- Anderson DM, Overpeck JT, Gupta AK (2002) Increase in the Asian Southwest Monsoon during the past four centuries. *Science* 297:596–599. doi:10.1126/science.1072881
- Behera SK, Luo J-J, Masson S (2005) Paramout impact of the Indian Ocean Dipole on the East African short rains: a CGCM study. *J Clim* 18:4514–4530. doi:10.1175/JCLI3541.1
- Bergonzini L, Richard Y, Petit L, Camberlin P (2004) Zonal circulation over the Indian and Pacific Oceans and the levels of Lakes Victoria and Tanganyika. *Int J Climatol* 24:1613–1624. doi:10.1002/joc.1089
- Birkett C, Murtugudde R, Allan T (1999) Indian Ocean climate event brings flood to East Africa's lakes and the Sudd Marsh. *Geophys Res Lett* 26:1031–1034. doi:10.1029/1999GL900165
- Black E, Slingo J, Sperber KR (2003) An observational study of the relationship between excessively strong short rains in coastal East Africa and Indian Ocean SST. *Mon Weather Rev* 131:74–94. doi:10.1175/1520-0493(2003)131<0074:AOSOTR>2.0.CO;2
- Brohan P, Kennedy JJ, Harris I, Tett SFB, Jones PD (2006) Uncertainty estimates in regional and global observed temperature changes: a new dataset from 1850. *J Geophys Res* 111. doi:10.1029/2005JD006548
- Burns SJ, Fleitmann D, Mudelsee M, Neff U, Matter A, Mangini A (2002) A 780 yr annually-resolved record of Indian Ocean monsoon precipitation from a speleothem from south Oman. *J Geophys Res* 107. doi:10.1029/2001JD001281

- Charles CD, Hunter DE, Fairbanks RG (1997) Interaction between the ENSO and the Asian Monsoon in a coral record of tropical climate. *Science* 277:925–928. doi:[10.1126/science.277.5328.925](https://doi.org/10.1126/science.277.5328.925)
- Charles CD, Cobb K, Moore MD, Fairbanks RG (2003) Monsoon-tropical ocean interaction in a network of coral records spanning the 20th century. *Mar Geol* 201:207–222. doi:[10.1016/S0025-3227\(03\)00217-2](https://doi.org/10.1016/S0025-3227(03)00217-2)
- Chelliah M, Bell GD (2004) Tropical Multidecadal and inter-annual climate variability in the NCEP-NCAR reanalysis. *J Clim* 17:1777–1803. doi:[10.1175/1520-0442\(2004\)017<1777:TMAICV>2.0.CO;2](https://doi.org/10.1175/1520-0442(2004)017<1777:TMAICV>2.0.CO;2)
- Cherchi A, Gualdi S, Behera S, Luo JJ, Masson S, Yamagata T et al (2007) The influence of tropical Indian Ocean SST on the Indian Summer Monsoon. *J Clim* 20:3083–3105. doi:[10.1175/JCLI4161.1](https://doi.org/10.1175/JCLI4161.1)
- Clark CO, Cole JE, Webster PW (2000) Indian Ocean SST and Indian summer rainfall: predictive relationships and their decadal variability. *J Clim* 13:2503–2519. doi:[10.1175/1520-0442\(2000\)013<2503:IOSAIS>2.0.CO;2](https://doi.org/10.1175/1520-0442(2000)013<2503:IOSAIS>2.0.CO;2)
- Clark CO, Webster PJ, Cole JE (2003) Interdecadal variability of the relationship between the Indian Ocean Zonal Mode and east African coastal rainfall anomalies. *J Clim* 16:548–554. doi:[10.1175/1520-0442\(2003\)016<0548:IVOTRB>2.0.CO;2](https://doi.org/10.1175/1520-0442(2003)016<0548:IVOTRB>2.0.CO;2)
- Cobb KM, Charles CD, Hunter DE (2001) A central tropical Pacific coral demonstrates Pacific, Indian, and Atlantic decadal climate connections. *Geophys Res Lett* 28:2209–2212. doi:[10.1029/2001GL012919](https://doi.org/10.1029/2001GL012919)
- Cohen AS, Lezzar KE, Cole J, Dettman D, Ellis GS, Gonneea ME et al (2006) Late Holocene linkages between decade-century scale climate variability and productivity at Lake Tanganyika, Africa. *J Paleolimnol* 36:189–209. doi:[10.1007/s10933-006-9004-y](https://doi.org/10.1007/s10933-006-9004-y)
- Cole JE, Dunbar RB, McClanahan TR, Muthiga NA (2000) Tropical Pacific forcing of decadal SST variability in the Western Indian Ocean over the past two centuries. *Science* 287:617–619. doi:[10.1126/science.287.5453.617](https://doi.org/10.1126/science.287.5453.617)
- Cook ER, Krusic PJ, Jones PD (2003) Dendroclimatic signals in long tree-ring chronologies from the Himalayas of Nepal. *Int J Climatol* 23:707–732. doi:[10.1002/joc.911](https://doi.org/10.1002/joc.911)
- Dai A, Trenberth KE, Karl TR (1998) Global variations in droughts and wet spells: 1900–1995. *Geophys Res Lett* 25:3367–3370. doi:[10.1029/98GL52511](https://doi.org/10.1029/98GL52511)
- Damassa TD, Cole JE, Barnett HR, Ault TR, McClanahan TR (2006) Enhanced multidecadal climate variability in the seventeenth century from coral isotope records in the western Indian Ocean. *Paleoceanography* 21. doi:[10.1029/2005PA001217](https://doi.org/10.1029/2005PA001217)
- D'Arrigo R, Wilson R, Deser C, Wiles G, Cook E, Villalba R et al (2005) Tropical-North Pacific climate linkages over the past four centuries. *J Clim* 18:5253–5265. doi:[10.1175/JCLI3602.1](https://doi.org/10.1175/JCLI3602.1)
- D'Arrigo R, Wilson R, Li J (2006) Increased Eurasian-tropical temperature amplitude difference in recent centuries: Implications for the Asian Monsoon. *Geophys Res Lett* 33. doi:[10.1029/2006GL027507](https://doi.org/10.1029/2006GL027507)
- Davis ME, Thompson LG, Yao T, Wang N (2005) Forcing of the Asian monsoon on the Tibetan Plateau: evidence from high-resolution ice core and tropical coral records. *J Geophys Res* 110. doi:[10.1029/2004JD004933](https://doi.org/10.1029/2004JD004933)
- Deser C, Phillips AS, Hurrell JW (2004) Pacific Interdecadal climate variability: linkages between the tropics and the North Pacific during boreal winter since 1900. *J Clim* 17:3109–3124. doi:[10.1175/1520-0442\(2004\)017<3109:PICVLB>2.0.CO;2](https://doi.org/10.1175/1520-0442(2004)017<3109:PICVLB>2.0.CO;2)
- Fleitmann D, Burns SJ, Neff U, Mudelsee M, Mangini A, Matter A (2004) Palaeoclimatic interpretation of high-resolution oxygen isotope profiles derived from annually laminated speleothems from Southern Oman. *Q Sci Rev* 23:935–945. doi:[10.1016/j.quascirev.2003.06.019](https://doi.org/10.1016/j.quascirev.2003.06.019)
- Gershunov A, Schneider N, Barnett T (2001) Low-frequency modulation of the ENSO-Indian monsoon rainfall relationship: signal or noise? *J Clim* 14:2486–2492. doi:[10.1175/1520-0442\(2001\)014<2486:LFMOTM>2.0.CO;2](https://doi.org/10.1175/1520-0442(2001)014<2486:LFMOTM>2.0.CO;2)
- Goddard L, Graham NE (1999) Importance of the Indian Ocean for simulating rainfall anomalies over eastern and southern Africa. *J Geophys Res* 104:19099–19116. doi:[10.1029/1999JD900326](https://doi.org/10.1029/1999JD900326)
- Hastenrath S, Greischar L (1993) The monsoonal heat budget of the hydrosphere-atmosphere system in the Indian Ocean sector. *J Geophys Res* 98:6869–6881. doi:[10.1029/92JC02956](https://doi.org/10.1029/92JC02956)
- Hastenrath S, Polzin D (2005) Mechanisms of climate anomalies in the equatorial Indian Ocean. *J Geophys Res* 110. doi:[10.1029/2004JD004981](https://doi.org/10.1029/2004JD004981)
- Hoerling M, Hurrell J, Eischaid J, Phillips A (2006) Detection and attribution of 20th century northern and southern African rainfall change. *J Clim* 19:3989–4008. doi:[10.1175/JCLI3842.1](https://doi.org/10.1175/JCLI3842.1)
- Holmgren K, Karlén W, Lauritzen SE, Lee-Thorp JA, Partridge TC, Piketh S et al (1999) A 3000-year high-resolution stalagmite-based record of palaeoclimate for northeastern South Africa. *Holocene* 9:295–309. doi:[10.1191/095968399672625464](https://doi.org/10.1191/095968399672625464)
- Hugh MJ (2004) Near-surface zonal flow and east african precipitation receipt during austral summer. *J Clim* 17:4070–4079. doi:[10.1175/1520-0442\(2004\)017<4070:NZFAEA>2.0.CO;2](https://doi.org/10.1175/1520-0442(2004)017<4070:NZFAEA>2.0.CO;2)
- Hulme M, Osborn TJ, Johns TJ (1998) Precipitation sensitivity to global warming: comparison of observations with HadCM2 simulations. *Geophys Res Lett* 25:3379–3382. doi:[10.1029/98GL02562](https://doi.org/10.1029/98GL02562)
- Johnson TC, Barry SL, Chan Y, Wilkinson P (2001) Decadal record of climate variability spanning the past 700 yr in the southern tropics of East Africa. *Geology* 29:83–86. doi:[10.1130/0091-7613\(2001\)029<0083:DROCVS>2.0.CO;2](https://doi.org/10.1130/0091-7613(2001)029<0083:DROCVS>2.0.CO;2)
- Jury MR, Enfield DB, Mélice J-L (2002) Tropical monsoons around Africa: Stability of El Nino-Southern Oscillation associations and links with continental climate. *J Geophys Res* 107. doi:[10.1029/2000JC000507](https://doi.org/10.1029/2000JC000507)
- Jury MR, White WB, Reason CJC (2004) Modelling the dominant climate signals around southern Africa. *Clim Dyn* 23:717–726. doi:[10.1007/s00382-004-0468-z](https://doi.org/10.1007/s00382-004-0468-z)
- Kayanne H, Iijima H, Nakamura N, McClanahan T, Behera S, Yamagata T (2006) Indian Ocean Dipole index recorded in Kenyan coral annual density bands. *Geophys Res Lett* 33. doi:[10.1029/2006GL027168](https://doi.org/10.1029/2006GL027168)
- Krueger AC (1999) The influence of the decadal-scale variability of summer rainfall on the impact of El Nino and La Nina events in South Africa. *Int J Climatol* 19:59–68. doi:[10.1002/\(SICI\)1097-0088\(199901\)19:1<59::AID-JOC347>3.0.CO;2-B](https://doi.org/10.1002/(SICI)1097-0088(199901)19:1<59::AID-JOC347>3.0.CO;2-B)
- Kumar KK, Rajagopalan B, Cane MA (1999) On the weakening relationship between the Indian Monsoon and ENSO. *Science* 284:2156–2159. doi:[10.1126/science.284.5423.2156](https://doi.org/10.1126/science.284.5423.2156)
- Kumar A, Yang F, Goddard L, Schubert S (2004) Differing trends in the tropical surface temperatures and precipitation over land and oceans. *J Clim* 17:653–664. doi:[10.1175/1520-0442\(2004\)017<0653:DTITTS>2.0.CO;2](https://doi.org/10.1175/1520-0442(2004)017<0653:DTITTS>2.0.CO;2)
- Kuhnert H, Pätzold J, Wyrwoll K-H, Wefer G (2000) Monitoring climate variability over the past 116 years in coral oxygen isotopes from Ningaloo Reef, Western Australia. *Int J Earth Sci* 88:725–732. doi:[10.1007/s005310050300](https://doi.org/10.1007/s005310050300)
- Latif M, Dommenges D, Dima M, Grötzner A (1999) The role of Indian Ocean sea surface temperatures in forcing East African rainfall anomalies during December-January 1997/98. *J Clim* 12:3497–3504. doi:[10.1175/1520-0442\(1999\)012<3497:TROIOS>2.0.CO;2](https://doi.org/10.1175/1520-0442(1999)012<3497:TROIOS>2.0.CO;2)
- Mantua N, Hare S, Zhang Y, Wallace J, Francis R (1997) A Pacific interdecadal oscillation with impacts on salmon production. *Bull Am Meteorol Soc* 78:1069–1079. doi:[10.1175/1520-0477\(1997\)078<1069:APICOW>2.0.CO;2](https://doi.org/10.1175/1520-0477(1997)078<1069:APICOW>2.0.CO;2)

- Mason SJ (1995) Sea-surface temperature-south African rainfall associations, 1910–1989. *Int J Climatol* 15:119–135. doi:[10.1002/joc.3370150202](https://doi.org/10.1002/joc.3370150202)
- McCabe GJ, Palecki MA (2006) Multidecadal climate variability of global lands and oceans. *Int J Climatol* 26:849–865. doi:[10.1002/joc.1289](https://doi.org/10.1002/joc.1289)
- McPhaden MJ, Zebiak SE, Glantz MG (2006) ENSO as an integrating concept in Earth Science. *Science* 314:1740–1745. doi:[10.1126/science.1132588](https://doi.org/10.1126/science.1132588)
- Meehl GA, Hu A (2006) Megadroughts in the Indian Monsoon Region and Southwest North America and a mechanism for associated multidecadal Pacific sea surface temperature anomalies. *J Clim* 19:1605–1623. doi:[10.1175/JCLI3675.1](https://doi.org/10.1175/JCLI3675.1)
- Mercier F, Cazenave A, Maheu C (2002) Interannual lake level fluctuations (1993–1999) in Africa from Topex/Poseidon: connections with ocean-atmosphere interactions over the Indian Ocean. *Global Planet Change* 32:141–163. doi:[10.1016/S0921-8181\(01\)00139-4](https://doi.org/10.1016/S0921-8181(01)00139-4)
- Mutai CC, Ward MN (2000) East African rainfall and the Tropical circulation/convection on intraseasonal to interannual timescales. *J Clim* 13:3915–3939. doi:[10.1175/1520-0442\(2000\)013<3915:EARATT>2.0.CO;2](https://doi.org/10.1175/1520-0442(2000)013<3915:EARATT>2.0.CO;2)
- Owen RB, Crossley R, Johnson TC, Tweddle D, Kornfield I, Davison S et al (1990) Major low levels of Lake Malawi and their implications for speciation rates in cichlid fishes. *Proc R Soc Lond B Biol Sci* 240:519–553
- Parthasarathy B, Munot AA, Kothawale DR (1991) Indian summer monsoon rainfall indices: 1871–1990. *Meteorol Mag* 121:174–186
- Parthasarathy B, Munot AA, Kothawale DR (1995) Monthly and seasonal rainfall series for All-India homogeneous regions and meteorological subdivisions: 1871–1994. Contributions from Indian Institute of Tropical Meteorology, Research Report RP-065
- Pfeiffer M, Dullo W-C (2006) Monsoon-induced cooling of the western equatorial Indian Ocean as recorded in coral oxygen isotopes records from the Seychelles covering the period 1840–1994 AD. *Q Sci Rev* 25:993–1009. doi:[10.1016/j.quascirev.2005.11.005](https://doi.org/10.1016/j.quascirev.2005.11.005)
- Pfeiffer M, Timm O, Dullo W-C (2004) Oceanic forcing of interannual and multidecadal climate variability in the south-western Indian Ocean: evidence from a 160 year coral isotopic record (La Reunion, 50°E, 21°S). *Paleoceanography* 19. doi:[10.1029/2003PA000964](https://doi.org/10.1029/2003PA000964)
- Pfeiffer M, Timm O, Dullo W-C, Garbe-Schoenberg D (2006) Paired coral Sr/Ca and $\delta^{18}\text{O}$ records from the Chagos Archipelago: late twentieth century warming affects rainfall variability in the tropical Indian Ocean. *Geology* 34:1069–1072. doi:[10.1130/G23162A.1](https://doi.org/10.1130/G23162A.1)
- Poccard I, Janicot S, Camberlin P (2000) Comparison of rainfall structures between NCEP/NCAR reanalysis and observed data over tropical Africa. *Clim Dyn* 16:897–915. doi:[10.1007/s003820000087](https://doi.org/10.1007/s003820000087)
- Reason CJC (2001) Subtropical Indian Ocean SST dipole events and southern African rainfall. *Geophys Res Lett* 28:2225–2227. doi:[10.1029/2000GL012735](https://doi.org/10.1029/2000GL012735)
- Reason CJC (2002) Sensitivity of the southern African circulation to dipole sea-surface temperature patterns in the south Indian Ocean. *Int J Climatol* 22:377–393. doi:[10.1002/joc.744](https://doi.org/10.1002/joc.744)
- Reason CJC, Mulenga H (1999) Relationships between South African rainfall and SST anomalies in the southwest Indian Ocean. *Int J Climatol* 19:1651–1673. doi:[10.1002/\(SICI\)1097-0088\(199912\)19:15<1651::AID-JOC439>3.0.CO;2-U](https://doi.org/10.1002/(SICI)1097-0088(199912)19:15<1651::AID-JOC439>3.0.CO;2-U)
- Reason CJC, Rouault M (2002) ENSO-like decadal variability and South African rainfall. *Geophys Res Lett* 29. doi:[10.1029/2002GL014663](https://doi.org/10.1029/2002GL014663)
- Reason CJC, Allan RJ, Lindesay JA (1996) Evidence for the influence of remote forcing on interdecadal variability in the southern Indian Ocean. *J Geophys Res* 101:11876–11882. doi:[10.1029/96JC00122](https://doi.org/10.1029/96JC00122)
- Richard Y, Trzaska S, Roucou P, Rouault M (2000) Modification of the southern African rainfall variability/ENSO relationship since the late 1960's. *Clim Dyn* 16:883–895. doi:[10.1007/s003820000086](https://doi.org/10.1007/s003820000086)
- Ropelewski CF, Halpert MS (1987) Global and regional scale precipitation pattern associated with the El Niño/Southern Oscillation. *Mon Weather Rev* 115:1606–1626. doi:[10.1175/1520-0493\(1987\)115<1606:GARSPP>2.0.CO;2](https://doi.org/10.1175/1520-0493(1987)115<1606:GARSPP>2.0.CO;2)
- Saji HH, Goswami BN, Vinayachandran PN, Yamagata T (1999) A dipole mode in the tropical Indian Ocean. *Nature* 401:360–363
- Shi N, Chen L (2004) Evolution and features of global land June–August dry/wet periods during 1920–2000. *Int J Climatol* 24:1483–1493. doi:[10.1002/joc.1034](https://doi.org/10.1002/joc.1034)
- Smith TM, Reynolds RW (2003) Extended reconstruction of Global Sea Surface temperatures based on COADS data (1854–1997). *J Clim* 16:1495–1510. doi:[10.1175/1520-0442\(2003\)16<1228:ABTSAT>2.0.CO;2](https://doi.org/10.1175/1520-0442(2003)16<1228:ABTSAT>2.0.CO;2)
- Sontakke NA, Singh N (1996) Longest instrumental regional and all-India summer monsoon rainfall series using optimum observations: reconstruction and update. *Holocene* 6:315–331. doi:[10.1177/095968369600600306](https://doi.org/10.1177/095968369600600306)
- Stager JC, Ryves D, Cumming BF, Meeker LD, Beer J (2005) Solar variability and the levels of Lake Victoria, East Africa, during the last millenium. *J Paleolimnol* 33:243–251. doi:[10.1007/s10933-004-4227-2](https://doi.org/10.1007/s10933-004-4227-2)
- Tate E, Sutcliffe J, Conway D, Farquharson F (2004) Water balance of Lake Victoria: update to 2000 and climate change modelling to 2001. *J Hydrol Sci* 49:563–574. doi:[10.1623/hysj.49.4.563.54422](https://doi.org/10.1623/hysj.49.4.563.54422)
- Therrell MD, Stahle DW, Ries LP, Shugart HH (2006) Tree-ring reconstructed rainfall variability in Zimbabwe. *Clim Dyn* 26. doi:[10.1007/s00382-005-0108-2](https://doi.org/10.1007/s00382-005-0108-2)
- Thompson LG, Mosley-Thompson E, Davis ME, Henderson KA, Brecher HH, Zagorodnov VS et al (2002) Kilimanjaro Ice core records: evidence of Holocene climate change in Tropical Africa. *Science* 298:589–593. doi:[10.1126/science.1073198](https://doi.org/10.1126/science.1073198)
- Thompson LG, Mosley-Thompson E, Davis ME, Lin P-N, Henderson K, Mashiotta TA (2003) Tropical glacier and ice core evidence of climate change on annual to millennial time scales. *Clim Change* 59:137–155. doi:[10.1023/A:1024472313775](https://doi.org/10.1023/A:1024472313775)
- Timm O, Pfeiffer M, Dullo W-C (2005) Non-stationary ENSO-precipitation teleconnection over the equatorial Indian Ocean documented in a coral from the Chagos Archipelago. *Geophys Res Lett* 32. doi:[10.1029/2004GL021738](https://doi.org/10.1029/2004GL021738)
- Treydte KS, Schleser GH, Helle G, Frank DC, Winiger M, Haug GH et al (2006) The twentieth century was the wettest period in northern Pakistan over the past millenium. *Nature* 440:1179–1182. doi:[10.1038/nature04743](https://doi.org/10.1038/nature04743)
- Tyson PD, Cooper GRJ, McCarthy TS (2002) Millennial to multi-decadal variability in the climate of Southern Africa. *Int J Climatol* 22:1105–1117. doi:[10.1002/joc.787](https://doi.org/10.1002/joc.787)
- Vecchi GA, Harrison DE (2004) Interannual Indian Rainfall variability and Indian Ocean sea surface temperature anomalies. In: Wang C, Xie SP, Carton JA (eds) *Earth climate: the Ocean-Atmosphere Interaction*. AGU Geophysical Monograph Series 147, pp 247–259
- Verschuren D (2004) Decadal and century-scale climate variability in tropical Africa during the past 2000 years. In: Battarbee RW (ed) *Past Climate Variability through Europe and Africa*. Kluwer, Dordrecht
- Verschuren D, Laird KR, Cumming BF (2000) Rainfall and drought in equatorial east Africa during the past 1,100 years. *Nature* 403:410–414. doi:[10.1038/35000179](https://doi.org/10.1038/35000179)

- Webster PJ, Magana VO, Palmer TN, Shukla J, Tomas RA, Yanai M et al (1998) Monsoons: processes, predictability, and the prospects for prediction. *J Geophys Res* 103:14451–14510. doi: [10.1029/97JC02719](https://doi.org/10.1029/97JC02719)
- Williams CJR, Kniveton DR, Layberry R (2006) Climatic and oceanic associations with daily rainfall extremes over southern Africa. *Int J Climatol* 20. doi: [10.1002/joc.1376](https://doi.org/10.1002/joc.1376)
- Wilson R, Tudhope S, Brohan P, Osborn T, Briffa K, Tett S (2006) 250 years of reconstructed and modeled tropical temperatures. *J Geophys Res* 111. doi: [10.1029/2005JC003188](https://doi.org/10.1029/2005JC003188)
- Woodruff SD, Jenne RL, Slutz RJ, Steurer PM (1998) A comprehensive Ocean-Atmosphere data set. *Bull Am Meteorol Soc* 68:1239–1248. doi: [10.1175/1520-0477\(1987\)068<1239:ACOADS>2.0.CO;2](https://doi.org/10.1175/1520-0477(1987)068<1239:ACOADS>2.0.CO;2)
- Zinke J, von Storch H, Mueller B, Zorita E, Rein B, Mieding B, A - Eisenhauer- KIHZ-Consortium et al (2004a) Evidence for the climate during the Late Maunder Minimum from proxy data and model simulations available within KIHZ. In: von Storch H, Raschke E, Floeser G (eds) *The climate in historical times—towards a synthesis of Holocene proxy data and climate models*. Springer, Berlin
- Zinke J, Dullo W-C, Heiss GA, Eisenhauer A (2004b) ENSO and subtropical dipole variability is recorded in a coral record off southwest Madagascar for the period 1659 to 1995. *Earth Planet Sci Lett* 228:177–197. doi: [10.1016/j.epsl.2004.09.028](https://doi.org/10.1016/j.epsl.2004.09.028)
- Zinke J, Pfeiffer M, Timm O, Dullo W-C, Davies GR (2005) Atmosphere-Ocean dynamics in the western Indian Ocean recorded in corals. *Philos Trans R Soc A* 363:121–142. doi: [10.1098/rsta.2004.1482](https://doi.org/10.1098/rsta.2004.1482)